



RESEARCH ARTICLE

Holobiont Traits Shape Climate Change Responses in Cryptic Coral Lineages

Carsten G. B. Grupstra¹  | Kirstin S. Meyer-Kaiser²  | Matthew-James Bennett³  | Maikani O. Andres⁴ | David J. Juszkiwicz⁵  | James E. Fifer^{1,6}  | Jeric P. Da-Anoy¹  | Kelly Gomez-Campo⁷  | Isabel Martinez-Rugiero⁷  | Hannah E. Aichelman¹  | Alexa K. Huzar^{1,8}  | Annabel M. Hughes^{1,9}  | Hanny E. Rivera¹  | Sarah W. Davies¹ 

¹Department of Biology, Boston University, Boston, Massachusetts, USA | ²Biology Department, Woods Hole Oceanographic Institution, Woods Hole, Massachusetts, USA | ³MARE, Guia Marine Laboratory, Faculty of Sciences, University of Lisbon, Cascais, Portugal | ⁴Palau International Coral Reef Center, Koror, Palau | ⁵Coral Conservation and Research Group (CORE), Trace and Environmental DNA Laboratory (TrEnD), School of Molecular and Life Sciences, Curtin University, Bentley, Western Australia, Australia | ⁶Department of Ecology, Evolution, and Marine Biology, University of California San Diego, San Diego, USA | ⁷Department of Biology, The Pennsylvania State University, University Park, Pennsylvania, USA | ⁸Department of Integrative Biology, University of Texas at Austin, Austin, Texas, USA | ⁹Northeastern University Marine Science Center, Nahant, Massachusetts, USA

Correspondence: Carsten G. B. Grupstra (cgb.grupstra@fau.edu) | Sarah W. Davies (daviessw@bu.edu)

Received: 5 June 2024 | **Revised:** 20 September 2024 | **Accepted:** 25 September 2024

Funding: This work was supported by Division of Ocean Sciences, (2048589).

Keywords: chlorophyll | climate change | coral reefs | cryptic lineage | extreme reefs | light harvesting | microbiome | *Porites* | Symbiodiniaceae | thermal tolerance

ABSTRACT

As ocean warming threatens reefs worldwide, identifying corals with adaptations to higher temperatures is critical for conservation. Genetically distinct but morphologically similar (i.e. cryptic) coral populations can be specialized to extreme habitats and thrive under stressful conditions. These corals often associate with locally beneficial microbiota (Symbiodiniaceae photobionts and bacteria), obscuring the main drivers of thermal tolerance. Here, we leverage a holobiont (massive *Porites*) with high fidelity for C15 photobionts to investigate adaptive variation across classic (“typical” conditions) and extreme reefs characterized by higher temperatures and light attenuation. We uncovered three cryptic lineages that exhibit limited micro-morphological variation; one lineage dominated classic reefs (L1), one had more even distributions (L2), and a third was restricted to extreme reefs (L3). L1 and L2 were more closely related to populations ~4300 km away, suggesting that some lineages are widespread. All corals harbored *Cladocopium* C15 photobionts; L1 and L2 shared a photobiont pool that differed in composition between reef types, yet L3 mostly harbored unique photobiont strains not found in the other lineages. Assemblages of bacterial partners differed among reef types in lineage-specific ways, suggesting that lineages employ distinct microbiome regulation strategies. Analysis of light-harvesting capacity and thermal tolerance revealed adaptive variation underpinning survival in distinct habitats: L1 had the highest light absorption efficiency and lowest thermal tolerance, suggesting that it is a classic reef specialist. L3 had the lowest light absorption efficiency and the highest thermal tolerance, showing that it is an extreme reef specialist. L2 had intermediate light absorption efficiency and thermal tolerance, suggesting that it is a generalist lineage. These findings reveal diverging holobiont strategies to cope with extreme conditions. Resolving coral lineages is key to understanding variation in thermal tolerance among coral populations, can strengthen our understanding of coral evolution and symbiosis, and support global conservation and restoration efforts.

1 | Introduction

Corals are holobionts composed of host animals and diverse microbiota, including populations of photobionts in the family Symbiodiniaceae that provide energy from photosynthesis. Other microbiome members (bacteria, archaea, fungi, viruses, and various protists) also provide a range of services including nutrient cycling and protection from pathogens (Mohamed et al. 2023). Increasing temperatures associated with global climate change can disrupt partnerships between corals and their photobionts by compromising photosynthetic activity, which can trigger photobiont loss (Baird et al. 2009; Weis 2008) and disruption of bacterial communities (Vompe et al. 2024; Voolstra et al. 2024). The resultant nutritionally compromised “bleached” state can ultimately lead to mortality (Hughes et al. 2017). Coral bleaching events have become increasingly frequent and severe due to increased greenhouse gas emissions and local stressors (Donovan et al. 2020; Hughes et al. 2017), leading to the loss of 14% of coral reefs worldwide in under a decade (Souter et al. 2021). These events raise questions about whether coral reefs will persist in the future (Klein, Roch, and Duarte 2024), and if so, which adaptations and symbioses will facilitate survival.

“Extreme” coral reef habitats characterized by naturally higher mean temperatures (Schoepf et al. 2023) can serve as a space-for-time substitution to understand coral reef futures. These reefs can have higher daily mean temperatures than nearby “classic” reefs, yet they maintain relatively high coral cover (Schoepf et al. 2023). Extreme reefs select coral genotypes and microbiota that are able to persist in warmer waters, thereby acting as natural laboratories and providing potential for genetic rescue (Gonzalez et al. 2013). Some broad-level coral life-history traits (e.g., growth forms, growth rates, heterotrophy) are known drivers of coral thermal tolerance that can promote survival on extreme reefs (Burt et al. 2020; Camp et al. 2018; Darling et al. 2012). Additionally, given that photosynthesis disruption is at the core of the bleaching response, adaptations in light-harvesting traits of coral holobionts are also likely to underpin survival in high temperatures (Enríquez et al. 2017; Gómez-Campo, Enríquez, and Iglesias-Prieto 2022; Scheufen, Iglesias-Prieto, and Enríquez 2017; Scheufen, Krämer, Iglesias-Prieto, and Enríquez, 2017; Swain et al. 2018). However, less is known about how variation in these traits aligns with thermal tolerance among species with similar morphologies and life histories.

Recent sequencing efforts have uncovered many examples of cryptic (genetically distinct but morphologically similar) coral lineages that are structured across environmental gradients (e.g., light, temperature, reviewed in Grupstra et al. 2024). Some cryptic lineages are more abundant on extreme reefs and appear to have higher thermal tolerance than lineages inhabiting classic reefs (e.g., Rivera et al. 2022; Rose et al. 2021; Van Oppen et al. 2018), raising questions regarding the traits that underpin variation in thermal tolerance in such closely related and morphologically similar taxa. Cryptic lineages are also often associated with genetically distinct photobiont strains, species, or even genera that influence thermal tolerance (e.g., Durusdinium, Rose et al. 2021; Palacio-Castro et al. 2023; also see Johnston, Cunning, and Burgess 2022; Starko et al. 2023),

further complicating predictions of lineage responses to climate change.

The coral genus *Porites* Link, 1807 is particularly well suited for understanding the traits that underpin variation in thermal tolerance among cryptic lineages. Massive *Porites* corals (*Porites australiensis* Vaughan, 1918, *Porites lobata* Dana, 1846, and *Porites lutea* Milne Edwards & Haime, 1851) are major reef builders across the Pacific Ocean, and they inhabit classic and extreme reefs. Massive *Porites* exhibit high fidelity for *Cladocopium* C15 photobionts via vertical transmission (Bennett et al. 2024; Forsman et al. 2020). Due to this tight partnership, variation in thermal tolerance among lineages is likely the result of local adaptation in the host, combined with strain-level variation in photobiont associations and interactions between other important holobiont members, such as bacteria (e.g., Ziegler et al. 2017). Bacterial communities of massive *Porites* are generally dominated by members of the family Endozoicomonadaceae, which can provide a variety of services to the coral holobiont, including nutritional benefits (Fifer et al. 2022; Pogoreutz and Ziegler 2024; Vompe et al. 2024). However, high temperatures can disrupt the partnership between *Porites* and Endozoicomonadaceae, resulting in shifts to less beneficial microbial communities (Vompe et al. 2024; but see Hadaidi et al. 2017).

Taxonomy of massive *Porites* is challenged by the high degree of variability of distinctive features for differentiating species (Brakel 1977; Forsman et al. 2009). The genus contains several clades, each harboring one or more morphotypes (Forsman et al. 2009; Terraneo et al. 2021). Some morphotypes are also represented in multiple genetic clades, necessitating molecular tools to differentiate species or lineages (Forsman et al. 2009). Thus far, diverse genetically distinct, apparently cryptic, lineages of massive *Porites* have been identified throughout the Pacific basin (Afiq-Rosli et al. 2021; Boulay et al. 2014; Rivera et al. 2022; Starko et al. 2023; Tisthammer et al. 2020). Some of these lineages appear to be structured along environmental gradients (Boulay et al. 2014; Rivera et al. 2022; Tisthammer et al. 2020) and several differ in terms of thermal tolerance (Boulay et al. 2014; Rivera et al. 2022; Starko et al. 2023; but see Forsman et al. 2020). However, it remains unclear whether these lineages represent widely distributed described species, or whether they are localized taxa. It is also unknown to what extent differences in holobiont traits and symbiotic partnerships contribute to thermal tolerance.

Here, we identified colonies of three cryptic lineages of massive *Porites* that exhibit heterogeneous distributions across extreme and classic reef sites in Chelbacheb (The Rock Islands of Palau). Using these lineages, we aimed to answer five critical questions: (1) Do these lineages exhibit micromorphological characters that are consistent within current *Porites* taxonomy? (2) To what extent are they related to *Porites* lineages recently discovered elsewhere in the Pacific Ocean? (3) Do these lineages exhibit distinct symbioses? (4) Are these lineages functionally distinct? and (5) How do holobiont interactions shape thermal tolerance? Understanding how holobiont symbiosis and physiology interact to shape cryptic lineage distributions and thermotolerance is key to understanding how coral reefs will respond to future climate change.

2 | Materials and Methods

2.1 | Software

For the datasets described below, all data were analyzed in R v4.1.2 (R Core Team 2020). Linear models (LM) were fitted using the `lm` function in the package `stats` 4.1.2, and linear mixed-effects models (LMM) with the `lmer` function in `lme4` v1.1-31 (Bates et al. 2014); F-tests in `car` v3.0-12 were used for the selection of significant variables (Fox et al. 2019). Post hoc pairwise comparisons were conducted using `emmeans` v1.8.4-1 (Lenth et al. 2023). We assessed model assumptions using performance v0.10.2 (Lüdtke et al. 2021). Permutational multivariate ANOVAs (PERMANOVAs) were performed using the `adonis` function in `vegan` 2.6-4 (Oksanen et al. 2019).

2.2 | Site Selection and Sample Collection

Three extreme and three paired classic sites were selected in Chelbacheb, Palau (Figure 1A). Extreme sites were shallow semi-enclosed lagoons with high water retention, increased light attenuation, and distinct assemblages of massive *Porites* lineages compared to classic sites (Rivera et al. 2022; van Woesik et al. 2012). Between 2010 and 2018, these sites had naturally elevated water temperatures year-round (up to 2°C) compared to nearby classic sites. Seasonal temperature ranges at extreme sites were ~29°C–32°C, compared to ~28°C–31°C at classic sites (Rivera et al. 2022). Sites were selected to ensure that, aside from the contrast in terms of temperature between classic and extreme sites, variability was minimal: they were all comparable in terms of depth (1–6 m), proximity to land (~10–20 m from land), and wave exposure (calm, on the leeward side of the archipelago or in a lagoon).

Water temperatures were measured every 30 min using triplicate temperature loggers at each site (3–4 m depth) between November 2021 and May 2022, and light levels were measured with duplicate loggers for 16 days in April 2022 (Onset, Wareham, USA). Temperature and light data from each site were then averaged across replicate loggers. Colonies resembling the gross morphology of *Porites lobata* Dana, 1846 were tagged at all sites in November 2021 in a transect along the shoreline. All colonies were sampled between 1 and 6 m depth, with the majority between 3 and 4 m. All selected colonies were at least 1–5 m apart to reduce the risk of sampling clone mates while maximizing the probability that the colonies were exposed to similar conditions within a site. Targeted colonies were also relatively small in size (30–50 cm) to facilitate transportation to aquarium facilities for further analyses and experiments. The total area over which corals were collected was 250–500 m² per site. Tissue samples were taken from the center of each colony and immediately stored in ethanol at –20°C (2×2 cm samples; $n=90$ total, 15/site, Table S1). An additional 22 colonies were sampled in April 2022 ($n=2$ –7 per site, Table S1). We tested for differences in temperature (daily mean, maximum, minimum, and range) and light intensity levels (mean, maximum, range) between reef types (classic, extreme) using an LMM with individual sites included as a random effect.

2.3 | Coral Genetics and Micro-Morphological Observations

DNA was extracted from all samples and libraries were generated for population genetics approaches using 2b-RAD sequencing (Rippe et al. 2021; Wang et al. 2012) (see Supporting Methods). Note that 2b-RAD sequencing was conducted in two runs, but all population genetics metrics (F_{st} , admixture, principal component analysis) were generated based on 75 samples collected in November 2021 (out of 90) that were successfully sequenced in the first run. This approach revealed three genetically distinct lineages (L1–L3) of massive *Porites*. To uncover additional within-lineage population structure, we also reran the bioinformatics pipeline separately for each lineage with sufficient replication using the same settings (L1, $n=35$, L2, $n=31$). However, F_{st} values among within-lineage subpopulations were not calculated because of low replication ($n=3$ –15 per subpopulation), which can inflate F_{st} values due to fixed SNPs.

The entire 2021 dataset (all lineages) was then reanalyzed together with another recent 2b-RAD dataset that identified cryptic lineages of massive *Porites* in Kiritimati (Starko et al. 2023) to determine whether these represent different populations of the same lineages. Samples collected in Palau in April 2022 ($n=22$), as well as failed libraries from November 2021 ($n=15$), were sequenced in a later run using a reduced representation design and used for lineage assignment only (overall successful 2b-RAD sequencing $n=104/112$; Table S1). The combined data from the two sequencing runs were used to test the hypothesis that lineages differ in terms of their distributions across classic and extreme sites using a Chi-squared test. Then, micro-morphological analysis of skeletal fragments from Palau ($n=19$) was conducted to test whether the lineages were morphologically similar to any currently accepted *Porites* species (see Supporting Methods).

2.4 | Characterization of Microbial Communities

Characterization of photobiont and bacterial communities associated with each lineage was conducted on samples collected in November 2021 using ITS-2 and 16S sequencing, respectively (see Supporting Methods; Table S1). Raw ITS-2 reads were processed by Symportal (Hume et al. 2019) to produce defining intragenomic sequence variant (DIV) profiles for each coral colony (final $n=73$; Table S1). All colonies were dominated by C15 DIVs. Cumulative link mixed models (clmm) were used to test for differences in dominant C15 DIV associations. A null model was generated that included only site as a random effect, and a full model included an interaction between lineage and reef type, as well as site as a random effect. Two additional models included reef type or lineage as fixed effects, with site as a random effect. The function `anova.clmm` in `ordinal` v2022.11.16 was used for model selection, and `Anova.clmm` in `rcompanion` v.2.4.21 assessed effect sizes.

Quality filtering, denoising, merging, and taxonomy assignments of 16S rRNA gene reads were conducted with DADA2

against the *Silva* v. 138.1 database (Quast et al. 2012), and contaminant reads were removed in Phyloseq (McMurdie and Holmes 2013) (final $n = 48$; see Table S1, Supporting Methods). We tested for differences in bacterial diversity (Shannon and

Simpson indices, calculated based on the nonrarefied dataset using the `estimate_richness` function) using an LM with an interaction between lineage and reef type. Including site as a random effect resulted in model convergence failure, so it was

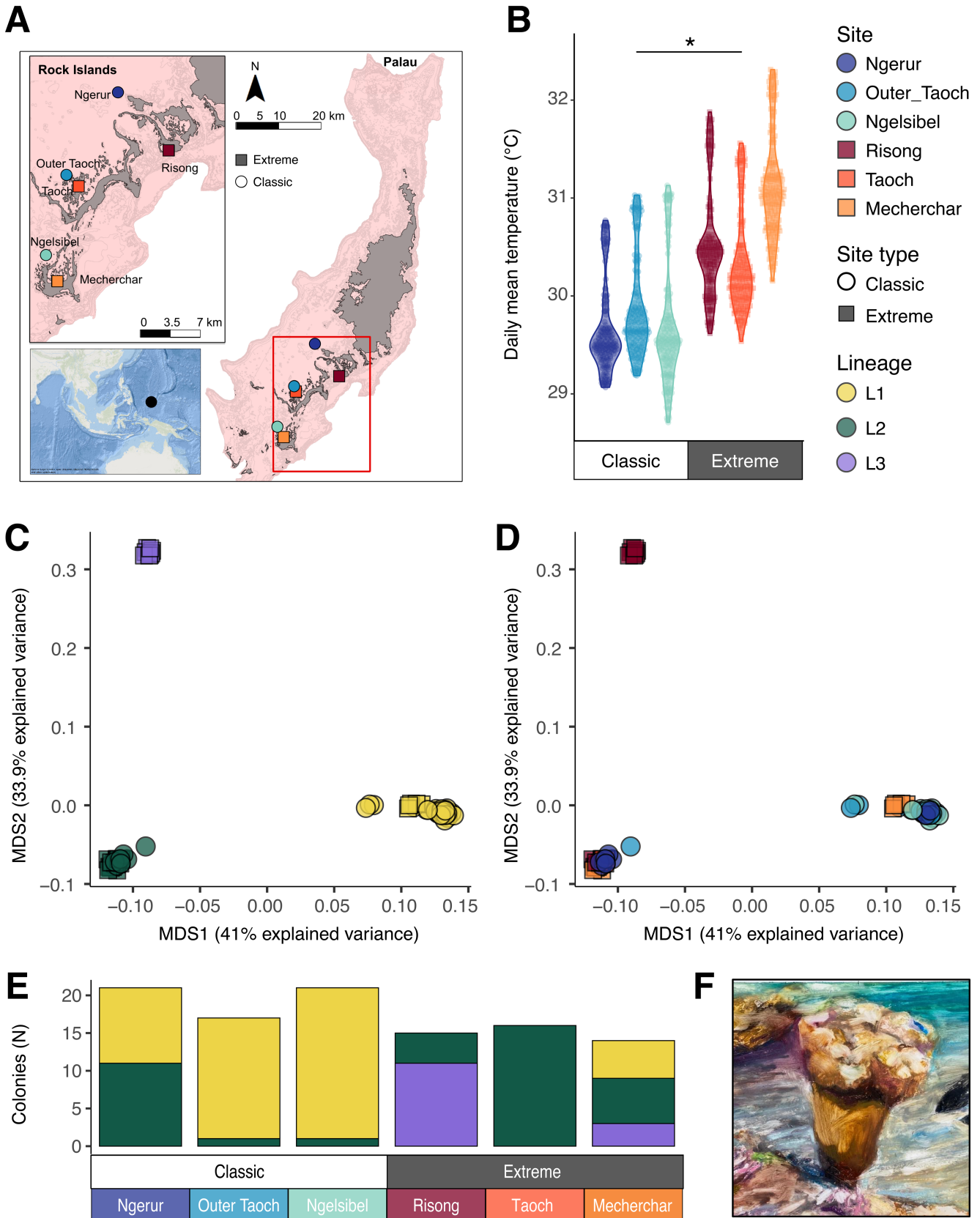


FIGURE 1 | Legend on next page.

FIGURE 1 | Collection sites, temperature conditions, and genetic structure of massive *Porites* at six study sites in Chelbacheb, Palau (Micronesia). (A) Three paired sites were selected ($n=6$ sites total), with each pair consisting of one exposed site (“classic reefs”, circles) and one enclosed lagoon site (“extreme reefs”, squares). (B) Daily mean temperatures between November 2021 and April 2022 were on average $\sim 1^\circ\text{C}$ higher at extreme sites ($30.7^\circ\text{C} \pm 0.6^\circ\text{C}$) relative to classic sites ($29.7^\circ\text{C} \pm 0.5^\circ\text{C}$, $F=13.3$, $p=0.02$). (C) MDS plots based on 2b-RAD data from samples collected in November 2021 ($n=487,248$ SNPs; see Table S1 for replication) revealed three genetic lineages (L1–L3) of massive *Porites*. (D) Same as C but with points colored by collection site. (E) Relative abundances of L1 (yellow) colonies were higher on classic reefs, whereas L2 (green) colonies had relatively even distributions among reef types; L3 (purple) colonies were restricted to extreme reefs. (F) Artistic representation of a massive *Porites* colony on an extreme reef in Chelbacheb, by Kimberly Collins Jermain. Lineages were identified via 2b-RAD sequencing across two sequencing runs ($n=104$ total, Table S1). See Figures S3 and S4 for additional detail on lineage classifications. Map lines delineate study areas and do not necessarily depict accepted national boundaries.

removed. Bray–Curtis distances were calculated based on data from which rare (< 10 reads) ASVs were removed (2361 remaining taxa). We tested for differences in bacterial community composition using a PERMANOVA with an interaction between lineage and reef type. To investigate site-level stochasticity in microbiome compositions, collection site was included in the model nested within reef type. Patterns of photobiont or bacterial communities among lineage subpopulations were visually explored but not statistically tested because subpopulations were structured nonrandomly among sites and reef types, impeding unbiased comparisons.

2.5 | Analyses of Holobiont Optical Traits

To characterize differences in holobiont structural and optical traits, we quantified polyp densities and light-harvesting characteristics in a subset of coral colonies (Table S1; Supporting Methods). A total of 20 tagged colonies of known lineage and reef type (Table S1) were transported to Boston University in May 2023, fragmented, and then acclimated for 63 days in aquariums. Reflectance (R) between 400 and 750 nm was measured (*sensu* Enríquez, Méndez, and Iglesias-Prieto 2005; Vásquez-Elizondo et al. 2017) (see Supporting Methods). Chlorophyll *a* densities were quantified and the specific absorption coefficient of Chlorophyll *a* (Chl*a*; $a^*_{\text{chl}a}$), a measure of the light absorption efficiency of the holobiont, was estimated following Enríquez, Méndez, and Iglesias-Prieto (2005) (see Supporting Methods). We tested for differences in chlorophyll concentration and $a^*_{\text{chl}a}$ values among lineages using an LM with reef type and lineage as fixed effects (no interaction because we only had L2 colonies from both reef types). Pairwise comparisons among lineages were conducted with a Bonferroni *p*-value correction.

2.6 | Thermal Challenge Experiment

A 25-day common garden heat challenge experiment was conducted to test for differences in thermal tolerance between the three *Porites* lineages ($n=24$; Table S1; see Supporting Methods). L1 colonies were collected from classic reefs and L2 and L3 colonies were collected from extreme reefs. We initially aimed to include L1 and L2 colonies from both extreme and classic reefs, but were unsuccessful. Two cores were extracted from each colony; one core was assigned to the control treatment, and the other to the heat treatment. Mean temperatures in control tanks

($n=3$ tanks per treatment) were maintained at $29.5^\circ\text{C} \pm 0.1^\circ\text{C}$. Temperatures in the heat treatment tanks were ramped by $\sim 3^\circ\text{C}$ over 7 days, followed by a 12-day hold. On day 19, temperatures were increased by an additional $\sim 1^\circ\text{C}$ to simulate an extreme thermal stress event until day 25. All cores were inspected daily for mortality. Maximum PSII photochemical efficiency (F_v/F_m) was measured daily or semi-daily following > 90 min of dark incubation. All fragments were also photographed with a color standard at six timepoints to measure changes in coloration (paling), quantified as the intensity in the gray channel using ImageJ (*sensu* McLachlan and Grottolli 2021). To control for differences in gray intensity at the start of the experiment, we also calculated and analyzed relative changes in gray intensity (Δ grey intensity; values in heat-values in control for each colony at each timepoint).

Lineage-specific survival rates were estimated with the Kaplan–Meier method and a *G*-test using the packages survival v3.3–1 (Therneau 1999) and survminer v0.4.9 (Kassambra 2018). To test how lineage and thermal challenge affected F_v/F_m and coloration of coral colonies over time, we used an LMM with a three-way interaction between treatment, lineage, and time. Colony number was included as a random effect to account for repeated sampling. Photobiont DIV was not included in the models because it co-varied with lineage. For relative coloration, the same analysis was done but treatment was not included in the analysis (because the values for heat-treated corals were relative to controls). Post hoc pairwise comparisons between lineages for each day across treatments were conducted with a Sidak (F_v/F_m between treatments), false discovery rate (F_v/F_m between lineages and grey intensity), or Bonferroni (Δ grey intensity) correction.

3 | Results

3.1 | Extreme Sites are Characterized by Higher Mean Temperatures

Over the study period, daily mean, maximum, and minimum temperatures were 0.8°C – 1.1°C higher at extreme sites (Figure 1B, Figure S1) than at paired classic sites (LMM results: $F=13.3$, $p=0.02$; $F=25.9$, $p=0.01$; $F=9.1$, $p=0.04$). Daily temperature range did not differ between extreme and classic sites (Figure S1). Light intensities (mean, maximum, range) also did not differ between reef types over the 16-day measurement period (Figure S2).

3.2 | Uneven Distributions of Lineages Between Reef Types

SNP data revealed three distinct genetic lineages (henceforth L1, L2, L3) in Palau (Figure 1C, Figures S3, S4). Including only samples collected in 2021 (Table S1), weighted F_{ST} values using all loci (487,248 loci) were 0.286 between L1 (yellow) and L2 (green), 0.468 between L1 and L3 (purple), and 0.456 between L2 and L3. When only neutral loci were included (outliers removed), F_{ST} values dropped to 0.12 between L1 and L2 (based on 844,221 loci, after 5882 outlier loci were removed), 0.29 between L1 and L3 (purple; 765,683 loci, 5521 loci removed), and 0.28 between L2 and L3 (793,557 loci, 5797 loci removed). Relative abundances of the three lineages (including samples sequenced in a subsequent run, $n=29$; Table S1) differed between classic and extreme sites ($\chi^2=50.3$, $p<0.001$). L1 colonies were more abundant at classic sites, while L2 exhibited more even distributions with higher abundances at extreme sites. L3 was restricted to two extreme sites (Risong and Mecherchar; Figure 1C).

Additional population genetic analysis within L1 and L2 revealed additional population structure (Figures S4–S6). Specifically, L1 appeared to be composed of four subpopulations (subpopulations A–D; Figure S5), and L2 of up to five (subpopulations E–I; Figure S6). However, intralineage population structure was relatively weak compared to primary lineage assignment, as indicated by low variation explained by MDS 1 (L1: 10.9%, L2: 6.8%) and MDS2 (L1: 8.9%, L2: 5.9%). Of note, populations of both lineages at Mecherchar were genetically distinct from other sites.

3.3 | Genetic Connectivity is Lower Among Co-Occurring Than Distant Lineages

A re-analysis of SNP data from Palauan samples from 2021 and data from Starko et al. (2023) showed that L1 and L2 are less genetically differentiated from lineages in Kiritimati than they are from co-occurring lineages in Palau (Figure S7; based on 13,443 loci). Specifically, L1 was more genetically similar to a lineage in Kiritimati (Pkir-2, $F_{ST}=0.16$) than to L2 or L3 ($F_{ST}=0.24–0.42$). Additionally, L2 was more genetically similar to another distinct lineage in Kiritimati (Pkir-1, $F_{ST}=0.22$) than to L1 or L3 ($F_{ST}=0.24–0.41$). L3 was highly differentiated from all other lineages, regardless of location ($F_{ST}=0.41–0.52$). A third Kiritimatian lineage (Pkir-3) was also highly diverged from all other lineages ($F_{ST}=0.38–0.52$), potentially indicating endemic lineages at both locations. Regardless, admixture analysis suggested that lineages in Palau and Kiritimati likely all represent reproductively isolated populations (Figure S8).

3.4 | Limited Micro-Morphological Traits Differentiate Some Lineages

Micro-morphological characterization from Z-stacked photos and SEM images from 19 coral fragments revealed morphological characters differentiating some lineages (Figure 2, see Supporting Results). However, due to morphological overlap among the three lineages, they are challenging to distinguish based on morphology alone. A key distinctive feature of L1 (Figure 2A–D) is the occasional fusion of the ventral directive

to the lateral septa of the triplet, resulting in a large palus almost equal in size to the pali of the lateral pairs (Figure 2D). The morphological characteristics closely resemble those of *Porites australiensis* Vaughan, 1918, with similarities to *Porites lutea* Milne Edwards & Haime, 1851. However, the absence of frequent triplet fusion or trident formation suggests a closer affinity with the former.

L2 (Figure 2E–H) and L3 (Figure 2I–L) can be distinguished from L1 because they lack fusion of the ventral directive triplet observed in L1. Yet, they are challenging to distinguish from each other. The morphological characteristics of L2 and L3 both resemble those of *Porites lobata* Dana, 1846 but L3 shares some morphological similarities with L1 and *P. australiensis*, such as reduced length of the dorsal and ventral septum and well-formed pali usually larger or equal to the septal denticles.

3.5 | Photobiont Associations Differ Among Reef Types in Lineage-Specific Ways

All sampled colonies were dominated by *Cladocodium* C15 with 10 unique C15 DIVs identified (Figure 3). The full model (reef type \times lineage, with site as a random effect) provided the best fit of the data (full model AIC = 258.6, loglik = -115.3 df = 1, $p=0.002$, null model AIC = 264.4, loglik = -122.2). There was a significant interaction between lineage and reef type, but neither of the fixed effects were significant independently, indicating that photobiont populations differ among reef types in lineage-specific ways (Lineage LR $\chi^2=1.0$, df = 2, $p=0.60$; reef type LR $\chi^2=0.74$, df = 1, $p=0.39$; Lineage \times reef type, LR $\chi^2=9.43$, df = 2, $p=0.009$).

L1 and L2 shared a mostly common pool of photobiont DIVs, but relative abundances of DIVs differed among lineages and reef types. In contrast to L1 and L2, most ($n=8/10$) L3 colonies hosted unique C15 DIVs (C15.C15vp and C15.C15vp.C15vt) that were not found in the other lineages. Overall, C15.C15vn.C93a was the most observed DIV, which dominated L1 colonies at classic sites ($n=21/31$) and was also observed in L2 colonies at extreme sites ($n=4/22$). A different DIV was the most abundant at extreme sites, where it was found in all three lineages and associated with 50% of the colonies (C15.C93a, $n=18/36$), including all colonies of L1 ($n=4$). Of note, this DIV was only observed in one colony at classic sites (L2; out of 37 total colonies). While L1 colonies harbored distinct DIVs at extreme sites compared to classic sites, colonies of L2 hosted diverse DIVs at both reef types; three of these DIVs were shared between classic (out of four DIVs) and extreme sites (out of five DIVs). While replication is limited, and with the exception of four rare DIVs limited to two subpopulations, L1 and L2 subpopulations generally did not host distinct photobiont populations. The dominant DIV association also did not appear to be determined exclusively by site-level factors (see Supporting Results, Figures S9 and S10).

3.6 | Bacterial Communities Differ Among Lineages and Reef Types

Bacterial alpha diversity was higher in colonies sampled at extreme sites than at classic sites but did not differ among lineages

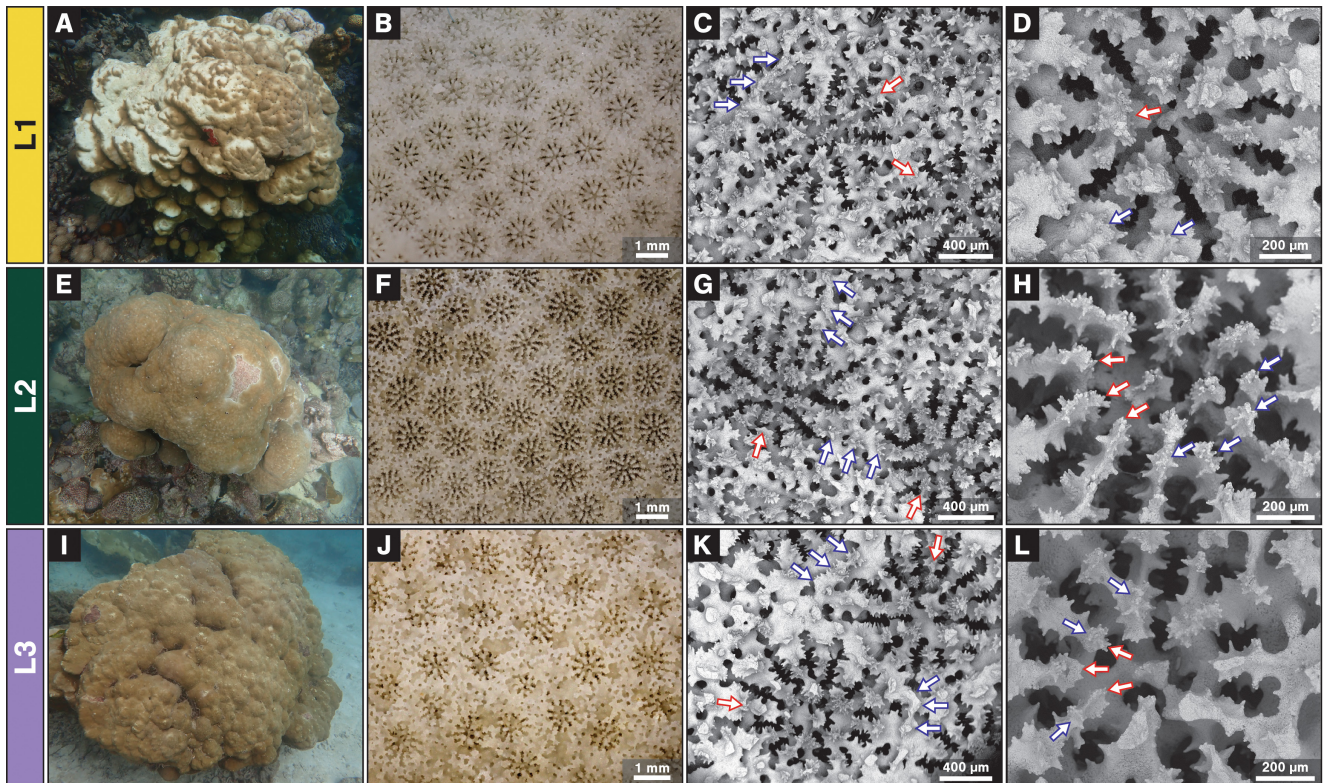


FIGURE 2 | In situ colonies and corallite morphology of *Porites* specimens collected from Palau, Micronesia, consisting of various representatives of L1 (A–D), L2 (E–H), and L3 (I–L). (A) Large colony with a series of thick ledges; (B) Corallites displaying thick straight walls and thick septa; (C) Corallites with a free ventral triplet (white–red outline arrows) and ridge-like walls with rough mural denticles (white–blue outline arrows); (D) Corallite with fusion of the ventral triplet, forming a large single palus (white–red outline arrow), with inner denticles smaller in size than the corresponding palus of the lateral pair septa (white–blue outline arrows); (E) Medium-sized hemispherical colony with a smooth appearance; (F) Corallites displaying moderately excavated calices with medium thick walls; (G) Corallites with a free ventral triplet (white–red outline arrows) and walls composed of three rows of denticles (white–blue outline arrows); (H) Corallite with free ventral triplet (white–red outline arrows) and inner denticles slightly more prominent or equal to the size of its corresponding septal palus (white–blue outline arrows); (I) Large hemispherical colony with a hillocky appearance; (J) Colony displaying moderately excavated calices with thick walls; (K) Corallites with a free ventral triplet (white–red outline arrows) and a ridge-like wall with rough granulated mural denticles (white–blue outline arrows); (L) Corallite with free ventral triplet (white–red outline arrows) and poorly developed pali smaller or equal to its corresponding septal denticle (white–blue outline arrows). (A, E, I) In situ colony images from Risong, depth 2–4 m; (B, F, J) Z-Stacked light microscope images; (C, D, G, H, K, L): SEM images of corallum surface.

(Figure 4A,B; Simpson LM results: Lineage $df=1$, $F=0.31$, $p=0.73$; Reef type: $df=1$, $F=7.11$, $p=0.01$, Lineage*Reef type: $df=1$, $F=3.13$, $p=0.084$; Shannon LM results: Lineage $df=2$, $F=0.21$, $p=0.81$; Reef type: $df=1$, $F=8.48$, $p=0.006$, Lineage*Reef type: $df=1$, $F=0.27$, $p=0.61$). Specifically, mean Simpson values were 1.17 (L2)–2.1 (L1) times higher and Shannon index values were 2.0 (L2)–2.3 (L1) times higher at extreme sites than classic sites.

Coral lineage was the most important driver of bacterial community compositions (Figure 4C, S11; $F=4.7$, $R^2=0.15$, $p=0.001$), followed by reef type ($F=4.1$, $R^2=0.07$, $p=0.002$). There were also significant interactions between lineage and reef type ($F=3.55$, $R^2=0.06$, $p=0.001$), and between lineage, reef type, and site ($F=1.8$, $R^2=0.11$, $p=0.016$). Dispersion was not significantly different among sampling groups ($df=4$, $F=1.92$, $p=0.12$). Of note, qualitative comparisons of bacterial communities among L1 and L2 subpopulations suggested that one L1 subpopulation at classic sites (C, $n=3$) hosted slightly different bacterial communities compared to other L1 subpopulations (Figures S12 and S13).

Most L1 and L2 colonies at classic sites were dominated by Endozoicomonadaceae (Figure 5A). At extreme sites, L2, but not L1 or L3, colonies also harbored substantial populations of this bacterial family. However, this was not statistically tested due to low replication and heterogeneous distributions of lineages at the site level. Lineages appeared to host distinct Endozoicomonadaceae ASVs (Figure 5B): L1 colonies at classic sites were dominated by ASV1, with many colonies also hosting ASV 6 ($n=15/24$) and 12 ($n=14/24$). L2 colonies at classic sites also all hosted ASVs 1 and 6, but only one colony at extreme sites hosted ASV 6. Most L2 colonies hosted ASV 10 instead of 12 ($n=14/16$), regardless of reef type, and half of L2 colonies at extreme sites also hosted ASV 20 ($n=5/10$). L1 and L3 colonies at extreme sites all hosted low abundances of ASV 1 ($n=8/8$).

3.7 | Optical Traits Differ Among Lineages

Lineages differed in terms of polyp densities (Figures 6A, S14, S15; see Supporting Results) and optical traits (Figure 6B–D).

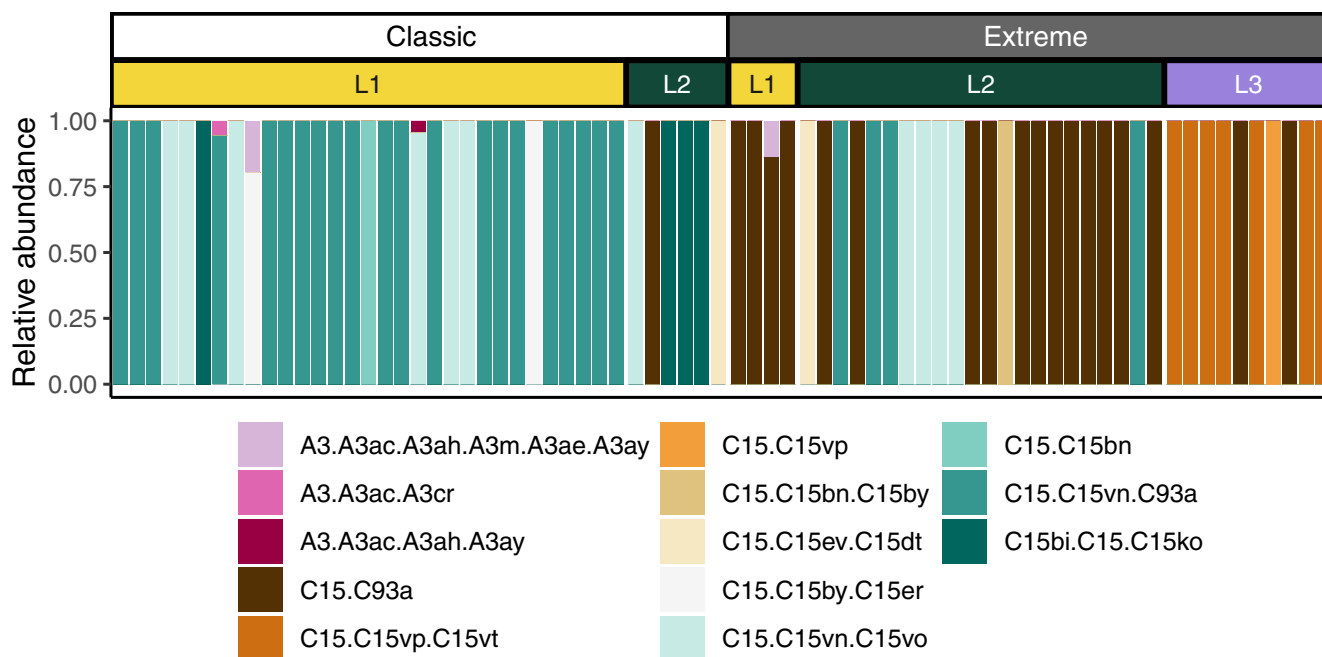


FIGURE 3 | Relative abundances of photobiont (Symbiodiniaceae) defining intragenomic variants (DIVs) across all three *Porites* lineages in classic and extreme reef types. All colonies were dominated by *Cladocopium* C15 DIVs. Note that one DIV is present in 50% of extreme reef colonies (C15.C93a, $n = 18/36$), while it was only found in one (out of 37) classic reef colony. Additionally, most ($n = 8/10$) L3 colonies hosted unique C15 DIVs (C15.C15vp and C15.C15vp.C15vt) not found in L1 or L2. Sample sizes (classic, extreme sites): L1 (31, 4); L2 (6, 22); and L3 (0, 10).

Chla densities (mean $\mu\text{g cm}^{-2} \pm \text{SE}$) varied among lineages (Figure 6B; $\text{df} = 2$, $F = 10.7$, $p = 0.001$) but not reef type ($\text{df} = 1$, $F = 1.3$, $p = 0.27$). L3 had the highest Chla concentrations (0.76 ± 0.06), followed by L2 (0.51 ± 0.04). L1 colonies had the lowest Chla concentrations (0.28 ± 0.06) (pairwise comparisons: L1–L2 est. = -0.29 , $\text{df} = 16$, $p = 0.023$; L1–L3 est. = -0.59 , $\text{df} = 16$, $p = 0.001$; L2–L3 est. = -0.30 , $\text{df} = 16$, $p = 0.01$).

Light absorption efficiency (α^*_{Chla} , $\text{m}^2 \text{mg chl}^{-1}$; Figure 6C) also varied among lineages ($\text{df} = 2$, $F = 5.9$, $p = 0.012$) but not reef type ($\text{df} = 1$, $F = 0.45$, $p = 0.51$). Pairwise comparisons (L1–L2 est. = 0.44 , $\text{df} = 16$, $p = 0.018$; L1–L3 est. = 0.60 , $\text{df} = 16$, $p = 0.016$; L2–L3 est. = 0.16 , $\text{df} = 16$, $p = 0.64$) showed that L1 had the highest α^*_{Chla} (0.74 ± 0.18), followed by L2 (0.36 ± 0.03). L3 had the lowest α^*_{Chla} (0.23 ± 0.01).

Plotting light absorption efficiency and chlorophyll *a* concentrations in the same figure (Figure 6D) visually demonstrated that the three lineages differ from one another in terms of optical traits; L3 colonies had low light efficiency, low risk, phenotypes; L1 colonies had high light efficiency, high risk, phenotypes; L2 colonies had intermediate phenotypes (sensu Scheufen, Iglesias-Prieto, and Enríquez 2017).

3.8 | Variation in Thermal Tolerance Among Lineages

Heat challenge affected coral survival, photosynthetic efficiency (F_v/F_m), and coloration; however, the strength of responses to heat differed among lineages (Table 1, Table S2; Figure 7 and Figure S16). Thermal challenge (Figure 7A) caused mortality in 46% ($n = 11/24$) of coral fragments

(Figure 7B). Mortality was first observed in L1 at day 12, and in L2 at day 16; mortality of L1 and L2 progressed until the end of the heat challenge. No mortality was observed in L3 ($n = 0/5$). Kaplan–Meier analysis demonstrated that survival rates significantly differed among the lineages (Figure 7B; $\chi^2 = 6$, $\text{df} = 2$, $p = 0.049$), and was lowest in L1 corals: full mortality was observed in 70% of L1 ($n = 7/10$), whereas only 44% of L2 colonies died ($n = 4/9$).

On day 1 of the heat challenge experiment, mean F_v/F_m values of the three lineages were similar, ranging between 0.608 ± 0.007 (L3) and 0.616 ± 0.005 (L2). Heat challenge significantly reduced F_v/F_m in all lineages (Figure 7C; Table 1); however, loss of F_v/F_m across lineages was significantly different (interaction between treatment and lineage) and the rate of loss varied significantly (interaction between treatment, lineage and day). For example, F_v/F_m values were reduced after just 5–6 days in L1 and L2, whereas L3 was not affected until day 14 (Table S3). Following this initial drop in F_v/F_m after 5–6 days, lineages exhibited different responses to the continued heat stress: F_v/F_m values continued lowering for L1 and L2 until day 10 of the experiment, whereas L3 remained stable and maintained significantly higher F_v/F_m values than L1 (Figure 7C; Table S4) and L2 (significant on day 10; L1–L3 est. = -0.091 , $p < 0.001$; L2–L3 est. = -0.06 , $p = 0.03$). F_v/F_m in L1 and L2 both showed some level of recovery between days 10 and 18, but this recovery was more pronounced for L2 (L1–L2 comparison at day 18; Figure 7C; Table S4). The compounded heat stress (days 19–25) caused further reductions in F_v/F_m values for all three lineages (Figure 7C), but L1 was more negatively affected than either of the other lineages (Tables S3 and S4). While not included in the model to avoid confounding effects, photobiont DIV also appeared to influence colony thermal tolerance, adding

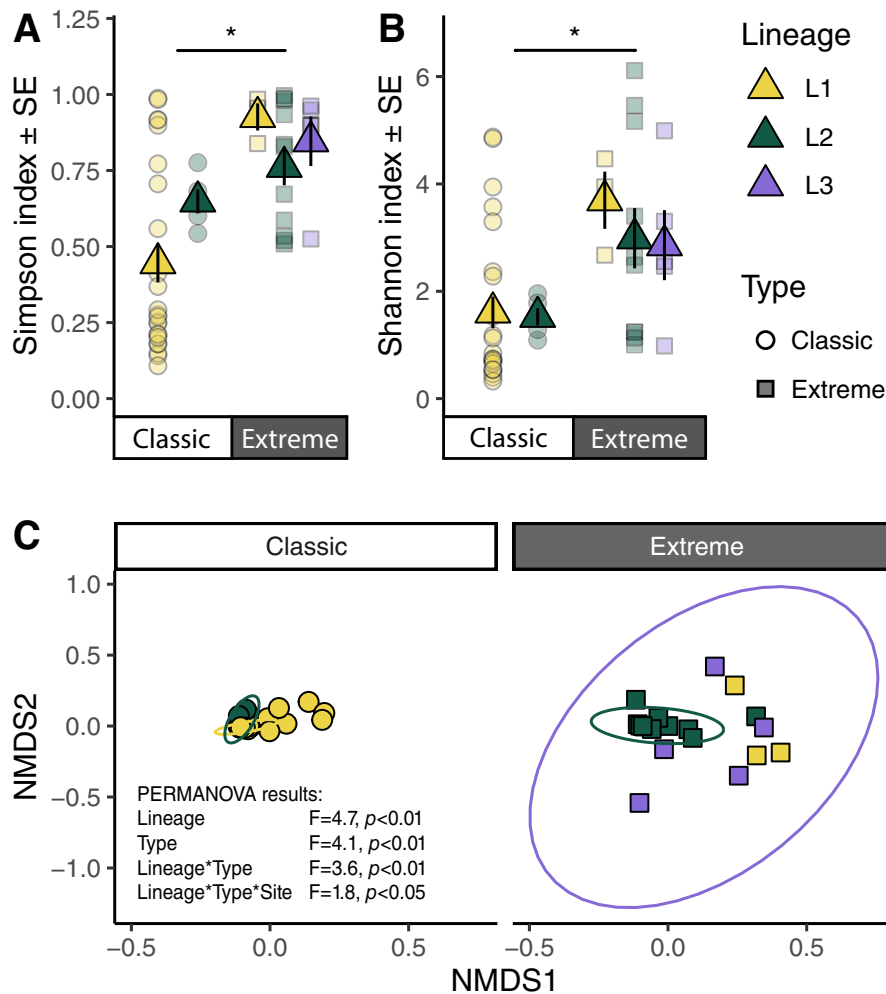


FIGURE 4 | Bacterial community compositions differ among lineages of massive *Porites* and reef types. Mean Simpson (A) and Shannon (B) metrics of bacterial diversity were significantly higher in corals sampled at extreme sites than in classic sites. (C) Nonmetric multidimensional scaling (NMDS) plots reveal differences in bacterial community compositions among lineages, reef types, and sites. NMDS stress=0.15. Ellipses denote 95% confidence interval. Sample sizes (classic, extreme sites): L1 (24, 3); L2 (5, 11); and L3 (0, 5).

an additional layer of complexity to lineage thermal responses (Figure S17).

Analysis of changes in grey intensity from standardized photographs showed that paling rates also differed among lineages (Figure S18; Table 1). Specifically, L1 colonies paled more rapidly than L2 or L3 (Figure S18; Table S5). For instance, post-hoc tests showed that L1 colonies were significantly more paled than L3 colonies at day 20 (higher Δ grey intensity; Table 1 and Table S6).

4 | Discussion

Scleractinian corals are morphologically and functionally diverse, but genetic and functional variation are often masked by morphological plasticity or similarity among sister taxa (Bongaerts et al. 2021; Boulay et al. 2014; Burgess et al. 2021; Grupstra et al. 2024). Understanding differences in thermal tolerance among morphologically indistinguishable—cryptic—coral lineages is key to predicting coral reef fates under warming futures. Yet, this understanding is further hindered

by heterogeneous associations with microbial partners that interact with host diversity to affect thermal tolerance (Palacio-Castro et al. 2023; Rose et al. 2021). Here, we provide strong evidence for three cryptic lineages (L1–L3) of a stony coral within the massive *Porites-Cladocopium* C15 system that exhibit high photobiont fidelity. In this system, cryptic lineages exhibit differential distributions across high-temperature extreme reefs versus more typical classic reefs (Figure 1). The uncovered lineages exhibit differences in their strain-level photobiont associations and bacterial community compositions. Lineages also differ in terms of optical traits, with those predominantly found in extreme reefs having lower light absorption efficiency (Figure 6). Together, these factors interacted to shape thermal tolerance; lineages typically observed on extreme reefs exhibited reduced paling and mortality during thermal challenge. Interestingly, we also observed interlineage variability in thermal tolerance within the extreme reefs, suggesting that host identity and holobiont composition are important drivers of thermal tolerance, regardless of environmental history (Figure 7). Together, these findings show that co-occurring cryptic coral lineages, although visually indistinguishable, can exhibit strong functional variation with

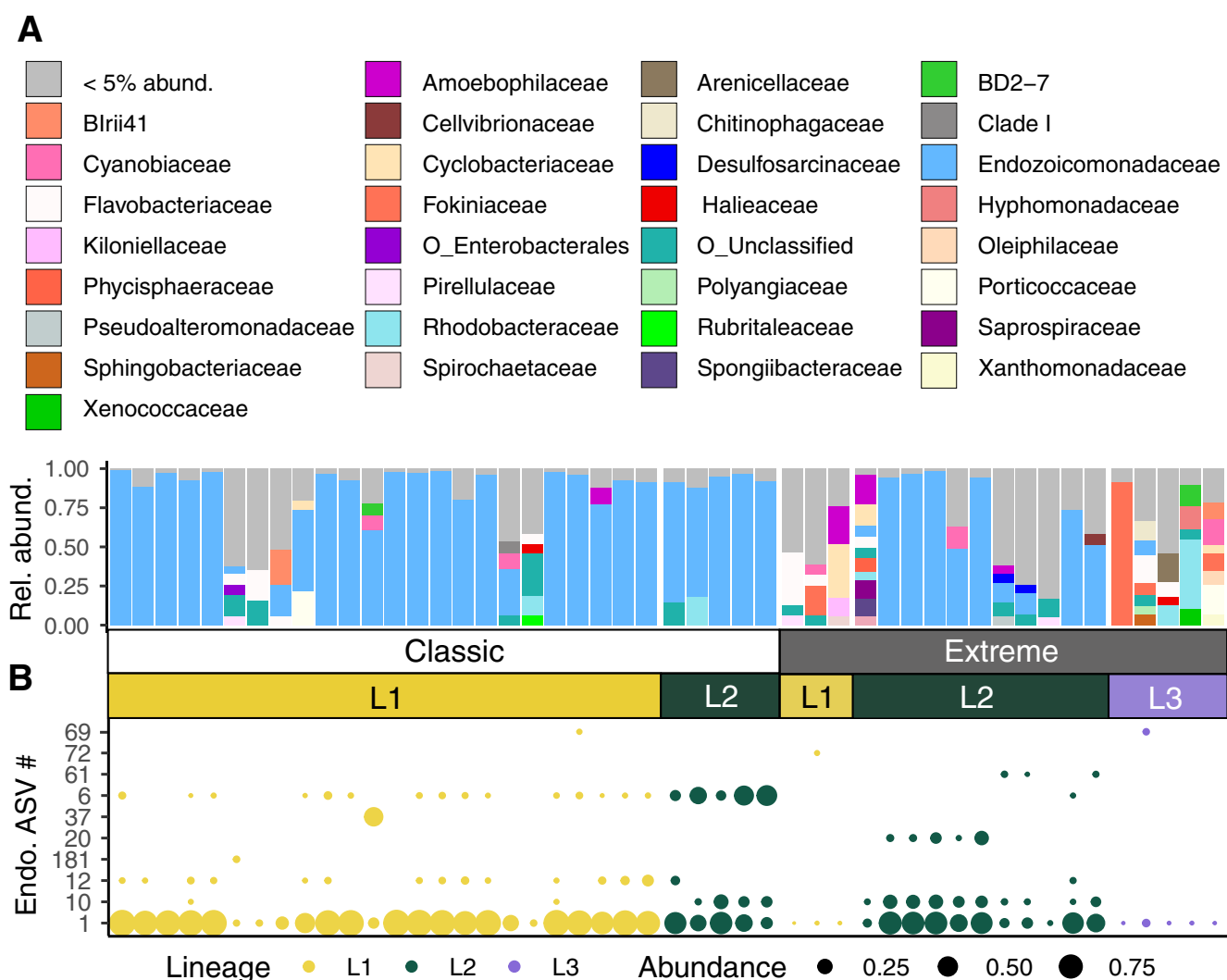


FIGURE 5 | Relative abundances of bacterial families associated with lineages of massive *Porites*. (A) Compositions of bacterial families differ among lineages and between reef types. Each bar represents an individual sample. Rel. abund. = relative abundance. (B) Relative abundances of the top 10 most abundant Endozoicomonadaceae ASVs. Endo. ASV# = Endozoicomonadaceae amplicon sequence variant number. Sample sizes (classic, extreme sites): L1 (24, 3); L2 (5, 11); and L3 (0, 5).

important implications for conservation and management under future climate change.

4.1 | Some Cryptic Lineages may Represent Widespread Species

The three identified cryptic lineages (L1–L3) of massive *Porites* differed in their relative abundances among classic and extreme reefs (Figure 1). Based on these distributions, we posit that L1 is a “classic” reef specialist, L2 is a generalist lineage, and L3 is an “extreme” reef specialist. Our sampling efforts support the findings of Rivera et al. (2022) that lineages of massive *Porites* differ in their distributions among Chelbacheb’s reefs. We infer that L1 is equivalent to the dark blue (DB) lineage in Rivera et al. (2022); L2 is equivalent to light blue (LB); and L3 is equivalent to red (RD). A fourth lineage (pink (PI)), reported by Rivera et al. (2022) to be more abundant at sites outside of the Rock Islands, was not represented in our study. Additionally, we find evidence for genetically distinct

subpopulations at some sites, which may indicate environmental selection or oceanographic barriers among some environments (Figures S4–S6). Combined with previous reports from across the Pacific Ocean, the data presented here show that lineages specialized to nearshore and offshore habitats (Afiq-Rosli et al. 2021; Boulay et al. 2014; Primov et al. 2024; Schweinsberg, Tollrian, and Lampert 2016; Tisthammer et al. 2020), as well as different depths (Voolstra et al. 2023), are a common feature on Pacific reefs.

Combined analysis of two 2b-RAD datasets showed that two of the Palauan lineages (L1 and L2) are more closely related to populations ~4300 km away in Kiritimati than to co-occurring lineages on the same reefs (Figure S7). Palau and Kiritimati each harbored lineages that were highly diverged from other sampled populations, suggesting that, while some cryptic *Porites* lineages may have wide distributions (i.e., L1 and L2 in Palau), others may be locally endemic (i.e., L3 in Palau). The levels of genetic differentiation observed between Palauan and Kiritimatian populations may reflect a

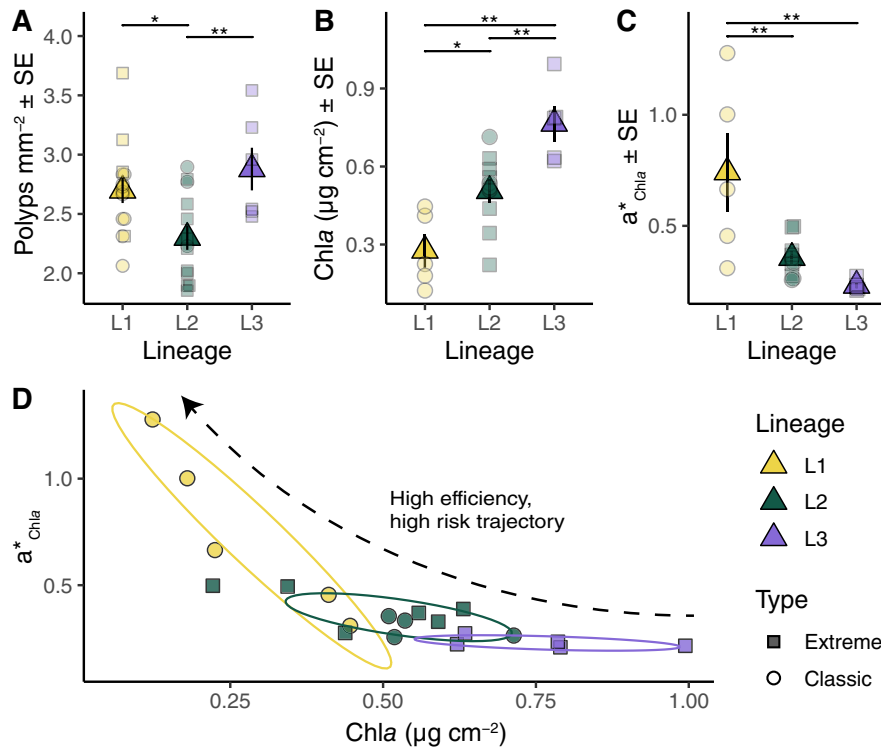


FIGURE 6 | Structural and optical traits of cryptic lineages of massive *Porites* in Palau indicate functional variation and specialization to classic and extreme reef environments. (A) Mean polyp densities (polyps mm^{-2}) differ among lineages. (B) Mean Chlorophyll *a* (Chla) concentrations ($\mu\text{g cm}^{-2}$) vary among lineages. (C) Mean Chla-specific absorption coefficient (a^*_{Chla} , $\text{m}^2 \text{mg chla}^{-1}$) values are higher in L1 than in the other lineages. (D) Higher Chla absorption (a^*_{Chla}) in L1 is correlated with lower Chla concentrations, which is a “high efficiency, high risk” phenotype (sensu Scheufen, Iglesias-Prieto, et al., 2017). Ellipses in (D) denote 68% confidence intervals. * $p < 0.05$, ** $p < 0.01$.

common pattern of isolation by distance in gonochoric broadcasting species (Aichelman and Barshis 2020; Nunes, Norris, and Knowlton 2011). Hence, we posit that L1 and Pkir-2, as well as L2 and Pkir-1, likely represent distinct populations of two lineages with limited gene flow. Based on morphological data (Figures 2 and 8), the L1-Pkir-2 lineage is likely most related to *P. australiensis*, and L2-Pkir-1 to *P. lobata*. L3 is an additional lineage that is also morphologically similar to *P. lobata*. Of note, while hybrid colonies were not found in this survey or in the recent work in Kiritimati (Starko et al. 2023), Rivera et al. (2022) did identify three adult colonies that were interlineage hybrids, suggesting that these lineages can hybridize to some extent.

Of interest, while L3 was the most genetically distant lineage, it was morphologically indistinguishable from L2 and challenging to distinguish from L1. This signals a decoupling of morphological and genetic differentiation, in line with previous surveys showing that samples matching the morphologies of *P. lobata*, *P. lutea*, *P. annae*, *P. solida*, and *P. harrisoni* together form a single clade in which morphotypes are genetically indistinguishable (Terraneo et al. 2021; but see Primov et al. 2024). Moreover, across Singaporean reefs, phylogenetic analyses of *Porites* could not resolve morphologically identified species, forming a complex that included *P. australiensis*, *P. lobata*, and *P. lutea* (Quek et al. 2023; Quek and Huang 2019). Further highlighting the taxonomic incongruencies among massive *Porites*, colonies matching the morphology of *P. lutea* were identified in three distinct genetic clades of *Porites* across the Pacific, and two in *P. lobata*

(Forsman et al. 2009). These phylogenomic analyses indicate that massive *Porites* consists of diverse species complexes, potentially each with plastic corallite morphologies. Yet, our findings suggest that morphological characteristics can, in some cases, still be useful for distinguishing genetic lineages. Broad-scale genetic sampling of morphologically similar colonies across various habitat types and depths coupled with skeletal morphology assessments by trained taxonomists is necessary to fully disentangle the taxonomy and distributions in Pacific massive *Porites*, as well as other coral genera.

4.2 | Locally Specialized and Lineage-Specific Photobiont Associations

Associations with distinct genera, species, or even strains of photobionts can have tremendous impacts on coral holobiont function and physiology (Howells et al. 2012; LaJeunesse et al. 2018; Thornhill et al. 2017). The potential for association with diverse photobionts may be limited among species of massive *Porites* given that they transmit photobionts maternally (Bennett et al. 2024; Forsman et al. 2020); however, local selection may aid the proliferation of suitable host-photobiont pairs in some environments (Prada et al. 2014; Prada and Hellberg 2021; Rippe et al. 2021). We found that all three *Porites* lineages in Palau harbored *Cladocopium* C15 photobionts, yet DIV (strain)-level variation was evident between classic and extreme reefs in lineage-specific ways.

TABLE 1 | Outputs of linear mixed-effects models for maximum photochemical efficiency (F_v/F_m), coloration (grey intensity), and relative coloration (Δ grey intensity: Heat–Control) during the heat challenge experiment.

Dependent variable	Independent variable	<i>F</i>	<i>df</i>	<i>p</i>
F_v/F_m	Treatment	946.2	1	<0.001
	Lineage	7.2	2	0.004
	Day	16.4	16	<0.001
	Treatment: lineage	15.1	2	<0.001
	Treatment: day	20.1	16	<0.001
	Lineage: day	1.3	32	0.101
	Treatment: lineage: day	2.1	32	<0.001
	Grey intensity	Treatment	241.9	1
	Lineage	15.5	2	<0.001
	Day	10.6	5	<0.001
	Treatment: lineage	7.4	2	<0.001
	Treatment: day	29.3	5	<0.001
	Lineage: day	0.9	10	0.496
	Treatment: lineage: day	0.7	10	0.743
Δ Grey intensity: H–C	Lineage	3.6	2	0.047
	Day	40.5	5	<0.001
	Lineage: day	0.9	10	0.495

Note: For all three models, coral colony (genotype) was included as a random effect. Significant *p*-values (<0.05) are bolded. Abbreviations: C, control; H, heat.

In contrast to our expectations, L1 and L2 predominantly shared a common pool of photosymbiont DIVs that differed between classic and extreme reefs (Figure 3, Figures S9, S10). For these lineages, photobiont associations did not appear to be driven by site-level factors or subpopulation structure (except for two subpopulations, Figures S9 and S10). On the other hand, most L3 colonies ($n = 7/10$) are associated with a unique DIV (C15.C15vp.C15vt) that was not observed in other lineages. This unique host–symbiont pairing is likely the result of vertical transmission (Forsman et al. 2020; Scott, Schott, and Matz 2024), supporting host–photobiont specialization. Similar variation in host–photobiont specificity at the strain level was identified among cryptic *Porites* lineages in Kiritimati (Starko et al. 2023), where one lineage hosted a distinct strain of C15 compared to the other lineages. However, a marine heatwave eroded this tight partnership, showing that abrupt environmental change can alter these associations (Starko et al. 2023).

Our results also suggest that some photobiont DIVs may be beneficial for the survival of massive *Porites* lineages on

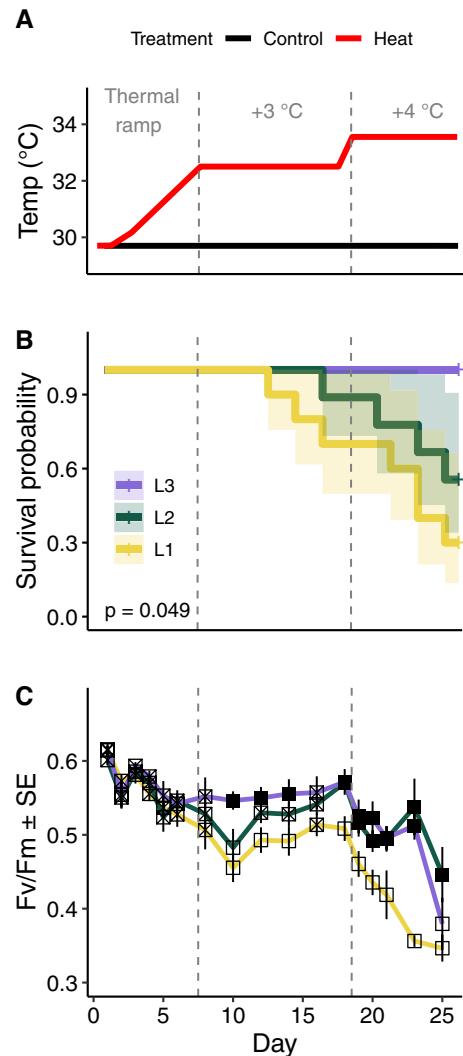


FIGURE 7 | Responses to thermal challenge differ among lineages of massive *Porites*. (A) Fragments of three lineages of massive *Porites* were distributed among control (~29.5°C) and heat tanks ($n = 3$ each) in which temperatures were raised by 3°C–4°C (see Figure S16 for measured temperatures). (B) Survival probability differed among lineages ($\pm 90\%$ CI) exposed to thermal challenge ($X^2 = 6$, $p = 0.049$). No mortality was observed in the control tanks. (C) Changes in photosynthetic efficiency (F_v/F_m) in colonies exposed to thermal challenge differed among lineages. Closed points differ significantly from open points ($p < 0.05$; see Table S4 for pairwise test results). Hatched points did not differ significantly from other points. Sample sizes: L1 ($n = 10$; seven died); L2 ($n = 9$; four died); and L3 ($n = 5$; zero died).

extreme reefs. For instance, DIV C15.C93a was common at extreme, but not classic, sites among colonies of all lineages (L1, $n = 4/4$; L2, $n = 12/22$; L3 $n = 2/10$), potentially indicating selection of locally beneficial host–photobiont pairings. Preliminary analysis of the effect of photobiont DIV on colony thermal tolerance in the thermal challenge experiment also suggests that colonies with this strain maintained higher F_v/F_m than colonies hosting other strains (Figure S17). However, additional work is needed to confirm this hypothesis. Alternatively, the observed patterns may simply indicate limited photobiont dispersal between extreme and classic sites (Golbuu et al. 2012).





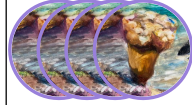







	L1		L2		L3	
Corallite morphology	<i>Porites cf. australiensis</i>		<i>Porites lobata</i>		<i>Porites cf. lobata</i>	
Putative subpopulations	Likely 4		Up to 5		None observed	
Reef type	Classic	Extreme	Classic	Extreme	Classic	Extreme
Relative abundance					-	
Photobiont associations	Variable	Only DIV C15.C93a	Variable	Mostly DIV C15.C93a	-	Mostly unique DIVs not found in other lineages
Microbiome	Dominated by Endo.	Variable	Dominated by Endo.	Dominated by Endo.	-	Variable
Light use efficiency		-			-	
Thermal tolerance		-	-		-	

FIGURE 8 | Overview of lineage traits examined in this study. Analysis of corallite morphology indicated subtle morphological differences among some lineages. Lineages differed in terms of their abundances (visualized as numbers of coral icons) and photobiont and bacterial associations between classic and extreme reefs. L1 and L2 also contained 4–5 putative subpopulations. Lineage-specific light use efficiency and thermal tolerance values are visualized using speedometers as low (pointing left), medium (pointing up), or high (pointing right). Note that L3 corals were not observed on classic reefs. Coral icons designed by Kimberly Collins Jermain. Endo: Endozoicomonadaceae.

4.3 | Microbiome Regulation Strategies Differ Among Lineages

Bacterial assemblages fulfill important services in coral holobionts, and association with locally beneficial bacteria can help corals respond to changing environments (Peixoto et al. 2021; Woolstra et al. 2024). Yet, corals differ in their potential to switch or shift between bacterial microbiome members, that is, microbiome flexibility, affecting their potential for acclimatization (Ziegler et al. 2019). We found that bacterial communities differed among cryptic lineages and reef types (Figures 4 and 5). Patterns of bacterial community assembly also differed between reef types in lineage-specific ways, suggesting differences in microbiome flexibility. For instance, L1 microbiomes were more variable at extreme sites than at classic sites whereas L2 colonies maintained relatively stable microbiomes regardless of reef type. Based on these findings, we posit that L1 is a microbiome conformer and L2 is a microbiome regulator (Ziegler et al. 2019). Microbiomes associated with L3 appeared highly variable and diverse, but given its limited distribution, it is not possible to disentangle whether this is a general feature of this lineage or the results of local stochasticity.

We observed that L1 and L3 colonies had low relative abundances of Endozoicomonadaceae at extreme sites compared to L2 colonies (Figure 5). Loss of this bacterial family has been documented in corals living in extreme environments and was attributed to environmental stress (Camp et al. 2020; Pantos

et al. 2015), but this has also been observed in corals regularly fed while living in captivity, potentially indicating reduced need for this putative nutritional symbiont (Barreto et al. 2021; Pogoreutz and Ziegler 2024). While paucity of Endozoicomonadaceae in the microbiomes of L1 and L3 may, thus, indicate microbiome disruption due to environmental stress, it could also indicate reduced need for this partner due to higher heterotrophic feeding in nearshore habitats with increased suspended particles (Anthony and Fabricius 2000; van Woesik et al. 2012). Alternatively, given the restricted distributions of L1 and L3 at extreme sites, these patterns could be partially explained by site-level stochasticity (Figure 5 and Figure S13). Future work investigating links between heterotrophy and Endozoicomonadaceae abundances among these lineages is warranted.

Individual Endozoicomonadaceae ASVs exhibited surprisingly heterogeneous distributions among lineages and reef types (Figure 5B). Some ASVs were more strongly associated with certain lineages (e.g., ASVs 10, 12, and 20), potentially indicating host specialization. Comparable patterns of host–lineage specialization were observed among Endozoicomonadaceae strains associated with genetically distinct populations of *Stylophora pistillata* at various locations (Buitrago-López et al. 2023; Neave et al. 2017). Some ASVs appeared to be more widely distributed and may, therefore, be cosmopolitan partners of massive *Porites* (e.g., ASV 1). Such widespread bacterial associations appear commonplace in corals that employ horizontal transmission of microbial communities and may indicate that some abundant

Endozoicomonadaceae ASVs are taken up from the environment (Neave et al. 2017). Other strains that were more abundant on one reef type (e.g., ASV6 on classic sites) may be more closely tied to the local environment than host lineage (i.e., classic sites in this study).

4.4 | Optical Adaptations of Holobiont Lineages to Distinct Reef Types

Corals receive most of their nutrition from their photobionts (Muscatine 1990). As a result, they have evolved mechanisms to optimize light harvesting in their environments (Enríquez, Méndez, and Iglesias-Prieto 2005; Enríquez et al. 2017; Terán et al. 2010). A common feature of cryptic coral lineages is that they are separated across habitats that differ in terms of light intensities, such as across depths or distance from shore (Grupstra et al. 2024), suggesting that they may be adapted to optimize local light conditions. Although we did not observe differences in light intensity between classic and extreme reefs over a 16-day measurement period in 2022 (Figure S2), previous work has shown that Palau's extreme reefs have higher light attenuation due to increased densities of suspended particles (van Woesik et al. 2012). Low light levels on Palau's extreme reefs have also been hypothesized to mitigate stress caused by high temperatures and result in the selection of low light-adapted coral species (van Woesik et al. 2012).

We found that lineages differed in terms of key traits correlated with light-harvesting strategies that can inform resistance to temperature and light stress. For instance, polyp density is associated with light scattering potential of the coral skeleton (Figure 6A; Gómez-Campo et al. 2024). Importantly, lineages differed in terms of Chla densities and light absorption efficiency (Figures 6 and 8). Low Chla concentrations coupled with high light absorption efficiency, as seen in L1, results in a reduction in self-shading of the photobiont cells and increased light scattering of the coral skeleton, which is commonly associated with high-light coral phenotypes and leads to higher energy production (Enríquez, Méndez, and Iglesias-Prieto 2005; Gómez-Campo, Enríquez, and Iglesias-Prieto 2022; Gómez-Campo et al. 2024). However, a reduction in self-shading also increases light stress in photobionts, raising bleaching probability in high temperatures. This combination of factors likely underpins why L1 is less abundant on extreme reefs where high temperatures increase photobiont stress, raising their probability of bleaching and mortality.

Low-light phenotypes, on the other hand, are generally characterized by higher Chla concentrations, which increases the likelihood of photon capture, but simultaneously results in higher chlorophyll self-shading, lower light absorption efficiency, and reduced total photosynthesis (Enríquez, Méndez, and Iglesias-Prieto 2005; Gómez-Campo, Enríquez, and Iglesias-Prieto 2022; Gómez-Campo et al. 2024; Mass et al. 2007; Winters et al. 2009). L3 colonies match these traits, and this likely explains why this lineage is restricted to extreme reefs: high Chla concentrations can be detrimental in high-light environments because of increased production of reactive oxygen species (ROS) that damage photobiont and host cells (Brown 1997; Cruz De Carvalho 2008; Weis 2008).

Reduced photosynthesis may also partially explain why L3 colonies have lower growth rates than colonies from co-occurring lineages (Rivera et al. 2022).

L2 colonies had intermediate levels of Chla and light absorption efficiency compared to L1 and L3, likely promoting survival in diverse habitats and supporting the hypothesis that this lineage is a habitat generalist. Of note, a lack of differences in Chla concentrations and light absorption efficiency among L2 colonies sampled in extreme and classic reefs (Figure 6) suggests that these traits may not be plastic, limiting the ability of massive *Porites* lineages to adjust to environmental change, and potentially resulting in the elimination of lineages not suitable for survival under future climate change conditions.

4.5 | Response Variation Among Holobiont Lineages to Thermal Challenge

Identifying adaptations and acclimatory mechanisms that shape responses to thermal challenge is critical to predicting the effects of rising ocean temperatures on coral communities and can aid restoration efforts (Barshis et al. 2018; Thomas et al. 2018). This is especially important for cryptic coral lineages that were assumed to be functionally similar (Grupstra et al. 2024). We found that distributions, holobiont compositions, and light absorption efficiency correlated with thermal tolerance in cryptic coral lineages, as tested using a common garden thermal challenge experiment (Figures 3–8). These lineage-specific thermotolerances are consistent with Rivera et al. (2022), who reported more stress bands during a bleaching event in 1988 in L1 (DB, 68%), relative to L2 (LB, 22%) and L3 (RD, 25%). Together, our findings suggest that extreme reefs select for locally beneficial holobionts with adaptive light harvesting traits that help corals delay bleaching under thermal challenge (Gómez-Campo, Enríquez, and Iglesias-Prieto 2022; Scheufen, Iglesias-Prieto, and Enríquez 2017; Scheufen, Krämer, Iglesias-Prieto, and Enríquez, 2017; Swain et al. 2016, 2018).

We also found critical differences between L2 and L3 in terms of mortality and F_v/F_m under thermal challenge, showcasing important response variation and distinct modes of holobiont adaptation among lineages exposed to similar environmental histories. It is likely that the factors that restrict L3 to extreme reefs, such as high fidelity for specific photobiont strains and increased specialization to low-light habitats (Figures 3–8), support its survivorship under thermal stress (Howells et al. 2012, 2020; Swain et al. 2016). On the other hand, association with more diverse photobiont strains, along with intermediate light harvesting efficiency, helps L2 live on diverse reef types, but this generalist strategy likely results in reduced survivorship of this lineage under thermal challenge. These findings also suggest that future marine heatwaves are likely to favor the survival of L3 compared to L2, warranting further investigation into the molecular mechanisms underpinning thermal tolerance in this lineage, and establishing this holobiont as an important resource for conservation and restoration efforts focused on reefs with high turbidity or sufficient shade.

One important remaining question is whether there are tradeoffs to the increased thermal tolerance in lineages of massive *Porites*.

For example, colonies of massive *Porites* from extreme mangrove habitat had lower gene expression variation, reduced skeletal density, and increased porosity compared to populations on “classic” reefs (Scucchia et al. 2023). In Palau, Rivera et al. (2022) found that L3 had lower skeletal density, calcification, and extension rates than the other lineages. Our findings also suggest that L3 may be less well equipped to handle light stress. Identifying such trade-offs in lineages with increased thermal tolerance will reveal important considerations for restoration efforts (but see Lachs et al. 2023).

It is also important to note the experimental design limitations in this study. The design of the thermal challenge experiment limits our ability to disentangle lineage and environment, given that all L1 colonies were collected from classic reefs whereas L2 and L3 colonies were collected from extreme reefs. We also did not control or measure light intensity during the experiment. Future experiments testing acclimatization to extreme reefs and host/photobiont genetics, for example, using reciprocal transplant experiments, will help disentangle these effects.

5 | Conclusions

Extreme reefs can offer a glimpse into the potential future for corals, revealing adaptations and microbial partnerships that can aid survival under future climate change conditions. Our findings suggest that extreme reefs with high temperatures and light attenuation promote associations with locally beneficial partners as well as the evolution and proliferation of optical traits that reduce light stress. Importantly, lineages appeared to employ distinct adaptations and acclimatory mechanisms to survive on extreme reefs, showing that there is no “one size fits all” mechanism that promotes survival. Some of the thermotolerant cryptic lineages discussed here, as well as in other recent works, may be suitable candidates for restoration efforts aimed to increase the abundances of thermally tolerant corals on reefs threatened by climate change. Slow-growing stress-tolerant species, such as massive *Porites* in particular, represent underutilized resources that can complement current restoration efforts (Guest et al. 2023).

Altogether, our findings emphasize the importance of resolving host genetic variation using molecular methods when conducting ecological experiments or determining “winners” and “losers” following bleaching events (Loya et al. 2001). L2 and L3 colonies are micromorphologically indistinguishable. Yet, response variation to thermal stress events among these lineages may result in heterogeneous mortality. Such differences in mortality among massive *Porites* lineages were recently reported in Kiritimati where one lineage experienced 75% mortality while overall mortality of the other lineages was only 20% (Starko et al. 2023). Our findings show that assemblages of *Porites* in the Pacific are composed of combinations of widespread and distinct local, potentially endemic, lineages. This suggests that heterogeneous responses to marine heatwaves are likely commonplace, potentially resulting in the elimination of yet unknown lineages. Combined with recent work showing comparable differences in thermal tolerance between cryptic lineages across the anthozoan tree of life (Grupstra et al. 2024), these findings demonstrate that cryptic diversity

is a key factor driving patterns of holobiont structuring as well as heterogeneous responses to ocean warming. Identifying and accounting for cryptic lineages is of key importance when quantifying phenotypic variation and planning restoration strategies.

Author Contributions

Carsten G. B. Grupstra: conceptualization, data curation, formal analysis, investigation, validation, visualization, writing – original draft, writing – review and editing. **Kirstin S. Meyer-Kaiser:** conceptualization, funding acquisition, investigation, project administration, resources, supervision, writing – original draft. **Matthew-James Bennett:** data curation, investigation, writing – review and editing. **Maikani O. Andres:** investigation, resources, writing – review and editing. **David J. Juszkiwicz:** formal analysis, methodology, writing – original draft, writing – review and editing. **James E. Fifer:** formal analysis, investigation, methodology, writing – original draft, writing – review and editing. **Jeric P. Da-Anoy:** formal analysis, investigation, writing – review and editing. **Kelly Gomez-Campo:** formal analysis, methodology, resources, writing – review and editing. **Isabel Martinez-Rugerio:** formal analysis, investigation, resources. **Hannah E. Aichelman:** formal analysis, investigation, writing – review and editing. **Alexa K. Huzar:** data curation, investigation, methodology. **Annabel M. Hughes:** investigation, methodology, writing – review and editing. **Hanny E. Rivera:** formal analysis, investigation, methodology, writing – review and editing. **Sarah W. Davies:** conceptualization, funding acquisition, project administration, resources, supervision, writing – original draft.

Acknowledgments

We would like to thank MJ Shanks for assistance with fieldwork and PICRC staff, including Joy Schnull-Sam, Louw Claassens, Arius Merep, and Rodney Kazuma for logistical support. Special thanks go out to Kimberly Collins Jermain for leading outreach activities with Palauan students and painting the artwork used in Figures 1 and 8. We also thank Justin Scace and Joel Sparks for their support with photography and SEM of coral skeletons, respectively. Members of the Coralassist lab are thanked for valuable discussions and insight. Davies lab members provided valuable feedback on the conducted analyses and figures. This study was made possible through a US National Science Foundation award to S.W.D. (OCE-2048589) and K.S.M.-K. (OCE-2048678), as well as Boston University start-up funds to S.W.D.

Ethics Statement

Sample collection was authorized by scientific research permits issued by the Palau Ministry of Natural Resources, Environment, and Tourism (RE-21-17, RE-22-17, RE-22-24, RE-23-09) and Koror State Government (69, 72, 78, and 83). Importation of coral samples to the United States was conducted with authorization from the Palau Bureau of Marine Resources and U.S. Fish and Wildlife Service (CITES permits PW22-042, PW22-162, PW23-089, PW23-090).

Conflicts of Interest

The authors declare no conflicts of interest.

Data Availability Statement

Raw host-targeted (2b-RAD) sequencing data were uploaded to the sequence read archive (SRA) under BioProject ID PRJNA1153969; microbiome-targeted sequencing data (ITS-2 rDNA and 16S rRNA gene amplicons) were uploaded under BioProject ID PRJNA1154296. All other data that support the findings of this study are openly available in Dryad at <https://doi.org/10.5061/dryad.1g1jwsv65>. All code data that support the findings of this study are openly available in Zenodo at

<https://doi.org/10.5281/zenodo.13992703> and GitHub at <https://github.com/grupstra-lab/Holobiont-specialization-in-massive-porites-lineages/tree/v1.0>.

References

- Afiq-Rosli, L., B. J. Wainwright, A. R. Gajanur, et al. 2021. “Barriers and Corridors of Gene Flow in an Urbanized Tropical Reef System.” *Evolutionary Applications* 14, no. 10: 2502–2515. <https://doi.org/10.1111/eva.13276>.
- Aichelman, H. E., and D. J. Barshis. 2020. “Adaptive Divergence, Neutral Panmixia, and Algal Symbiont Population Structure in the Temperate Coral *Astrangia poculata* Along the Mid-Atlantic United States.” *PeerJ* 8: e10201. <https://doi.org/10.7717/peerj.10201>.
- Anthony, K. R. N., and K. E. Fabricius. 2000. “Shifting Roles of Heterotrophy and Autotrophy in Coral Energetics Under Varying Turbidity.” *Journal of Experimental Marine Biology and Ecology* 252, no. 2: 221–253. [https://doi.org/10.1016/S0022-0981\(00\)00237-9](https://doi.org/10.1016/S0022-0981(00)00237-9).
- Baird, A. H., R. Bhagooli, P. J. Ralph, and S. Takahashi. 2009. “Coral Bleaching: The Role of the Host.” *Trends in Ecology & Evolution* 24, no. 1: 16–20. <https://doi.org/10.1016/j.tree.2008.09.005>.
- Barreto, M. M., M. Ziegler, A. Venn, et al. 2021. “Effects of Ocean Acidification on Resident and Active Microbial Communities of *Stylophora pistillata*.” *Frontiers in Microbiology* 12: 707674. <https://doi.org/10.3389/fmicb.2021.707674>.
- Barshis, D. J., C. Birkeland, R. J. Toonen, R. D. Gates, and J. H. Stillman. 2018. “High-Frequency Temperature Variability Mirrors Fixed Differences in Thermal Limits of the Massive Coral *Porites lobata* (Dana, 1846).” *Journal of Experimental Biology* 221, no. 24: 188581. <https://doi.org/10.1242/jeb.188581>.
- Bates, D. M., M. Maechler, B. Bolker, and S. Walker. 2014. “lme4: Mixed-Effects Modeling With R. R Package Version 1.1-7.” <http://CRAN.R-Project.Org/Package=lme4>.
- Bennett, M.-J., C. G. B. Grupstra, J. P. Da-Anoy, M. Andres, S. W. Davies, and K. S. Meyer-Kaiser. 2024. “Ex Situ Spawning, Larval Development, and Settlement in the Massive Reef-Building Coral *Porites lobata* in Palau.” *bioRxiv*: e12447. <https://doi.org/10.1101/ivb.12447>.
- Bongaerts, P., I. R. Cooke, H. Ying, et al. 2021. “Morphological Stasis Masks Ecologically Divergent Coral Species on Tropical Reefs.” *Current Biology* 31: 2286–2298. <https://doi.org/10.1101/2020.09.04.260208>.
- Boulay, J. N., M. E. Hellberg, J. Cortés, and I. B. Baums. 2014. “Unrecognized Coral Species Diversity Masks Differences in Functional Ecology.” *Proceedings of the Royal Society B: Biological Sciences* 281, no. 1776: 20131580. <https://doi.org/10.1098/rspb.2013.1580>.
- Brakel, W. H. 1977. “Corallite Variation in *Porites* and the Species Problem in Corals.” *Proceedings of the 3rd International Coral Reef Symposium*, 457–462. Panama.
- Brown, B. E. 1997. “Coral Bleaching: Causes and Consequences.” *Coral Reefs* 16: S129–S138.
- Buitrago-López, C., A. Cárdenas, B. C. C. Hume, et al. 2023. “Disparate Population and Holobiont Structure of Pocilloporid Corals Across the Red Sea Gradient Demonstrate Species-Specific Evolutionary Trajectories.” *Molecular Ecology* 32: 151–2173. <https://doi.org/10.1111/mec.16871>.
- Burgess, S. C., E. C. Johnston, A. S. J. Wyatt, J. J. Leichter, and P. J. Edmunds. 2021. “Response Diversity in Corals: Hidden Differences in Bleaching Mortality Among Cryptic *Pocillopora* Species.” *Ecology* 102, no. 6: e03324. <https://doi.org/10.1002/ecy.3324>.
- Burt, J. A., E. F. Camp, I. C. Enochs, et al. 2020. “Insights From Extreme Coral Reefs in a Changing World.” *Coral Reefs* 39, no. 3: 495–507. <https://doi.org/10.1007/s00338-020-01966-y>.
- Camp, E. F., V. Schoepf, P. J. Mumby, et al. 2018. “The Future of Coral Reefs Subject to Rapid Climate Change: Lessons From Natural Extreme Environments.” *Frontiers in Marine Science* 5: 4. <https://doi.org/10.3389/fmars.2018.00004>.
- Camp, E. F., D. J. Suggett, C. Pogoreutz, et al. 2020. “Corals Exhibit Distinct Patterns of Microbial Reorganisation to Thrive in an Extreme Inshore Environment.” *Coral Reefs* 39, no. 3: 701–716. <https://doi.org/10.1007/s00338-019-01889-3>.
- Cruz De Carvalho, M. H. 2008. “Drought Stress and Reactive Oxygen Species: Production, Scavenging and Signaling.” *Plant Signaling & Behavior* 3, no. 3: 156–165. <https://doi.org/10.4161/psb.3.3.5536>.
- Darling, E. S., L. Alvarez-Filip, T. A. Oliver, T. R. McClanahan, and I. M. Côté. 2012. “Evaluating Life-History Strategies of Reef Corals From Species Traits.” *Ecology Letters* 15, no. 12: 1378–1386. <https://doi.org/10.1111/j.1461-0248.2012.01861.x>.
- Donovan, M. K., T. C. Adam, A. A. Shantz, et al. 2020. “Nitrogen Pollution Interacts With Heat Stress to Increase Coral Bleaching Across the Seascape.” *Proceedings of the National Academy of Sciences of the United States of America* 117, no. 10: 5351–5357. <https://doi.org/10.1073/pnas.1915395117>.
- Enríquez, S., E. R. Méndez, O. Hoegh-Guldberg, and R. Iglesias-Prieto. 2017. “Key Functional Role of the Optical Properties of Coral Skeletons in Coral Ecology and Evolution.” *Proceedings of the Royal Society B: Biological Sciences* 284, no. 1853: 20161667. <https://doi.org/10.1098/rspb.2016.1667>.
- Enríquez, S., E. R. Méndez, and R. Iglesias-Prieto. 2005. “Multiple Scattering on Coral Skeletons Enhances Light Absorption by Symbiotic Algae.” *Limnology and Oceanography* 50, no. 4: 1025–1032. <https://doi.org/10.4319/lo.2005.50.4.1025>.
- Fifer, J. E., V. Bui, J. T. Berg, et al. 2022. “Microbiome Structuring Within a Coral Colony and Along a Sedimentation Gradient.” *Frontiers in Marine Science* 8: 805202. <https://doi.org/10.3389/fmars.2021.805202>.
- Forsman, Z. H., D. J. Barshis, C. L. Hunter, and R. J. Toonen. 2009. “Shape-Shifting Corals: Molecular Markers Show Morphology Is Evolutionarily Plastic in *Porites*.” *BMC Evolutionary Biology* 9, no. 45: 45. <https://doi.org/10.1186/1471-2148-9-45>.
- Forsman, Z. H., R. Ritson-Williams, K. H. Tisthammer, I. S. S. Knapp, and R. J. Toonen. 2020. “Host-Symbiont Coevolution, Cryptic Structure, and Bleaching Susceptibility, in a Coral Species Complex (Scleractinia; Poritidae).” *Scientific Reports* 10, no. 1: 16995. <https://doi.org/10.1038/s41598-020-73501-6>.
- Fox, J., S. Weisberg, B. Price, et al. 2019. “car: Companion to Applied Regression.” (Version 3.1–2) [Computer software]. <https://cran.r-project.org/web/packages/car/index.html>.
- Golbuu, Y., E. Wolanski, J. W. Idechong, et al. 2012. “Predicting Coral Recruitment in Palau’s Complex Reef Archipelago.” *PLoS One* 7, no. 11: e50998. <https://doi.org/10.1371/journal.pone.0050998>.
- Gómez-Campo, K., S. Enríquez, and R. Iglesias-Prieto. 2022. “A Road Map for the Development of the Bleached Coral Phenotype.” *Frontiers in Marine Science* 9: 806491. <https://doi.org/10.3389/fmars.2022.806491>.
- Gómez-Campo, K., R. Sanchez, I. Martínez-Rugiero, et al. 2024. “Phenotypic Plasticity for Improved Light Harvesting, in Tandem With Methylome Repatterning in Reef-Building Corals.” *Molecular Ecology* 33, no. 4: e17246. <https://doi.org/10.1111/mec.17246>.
- Gonzalez, A., O. Ronce, R. Ferriere, and M. E. Hochberg. 2013. “Evolutionary Rescue: An Emerging Focus at the Intersection Between Ecology and Evolution.” *Philosophical Transactions of the Royal Society, B: Biological Sciences* 368, no. 1610: 20120404. <https://doi.org/10.1098/rstb.2012.0404>.
- Grupstra, C. G. B., M. Gómez-Corrales, J. E. Fifer, et al. 2024. “Integrating Cryptic Diversity Into Coral Evolution, Symbiosis and

- Conservation." *Nature Ecology & Evolution* 8: 622–636. <https://doi.org/10.1038/s41559-023-02319-y>.
- Guest, J., M. V. Baria-Rodriguez, T. C. Toh, et al. 2023. "Live Slow, Die Old: Larval Propagation of Slow-Growing, Stress-Tolerant Corals for Reef Restoration." *Coral Reefs* 42, no. 6: 1365–1377. <https://doi.org/10.1007/s00338-023-02440-1>.
- Hadaidi, G., T. Röthig, L. K. Yum, et al. 2017. "Stable Mucus-Associated Microbial Communities in Bleached and Healthy Corals of *Porites lobata* From the Arabian Seas." *Scientific Reports* 7: 45362. <https://doi.org/10.1038/srep45362>.
- Howells, E. J., A. G. Bauman, G. O. Vaughan, B. C. C. Hume, C. R. Woolstra, and J. A. Burt. 2020. "Corals in the Hottest Reefs in the World Exhibit Symbiont Fidelity Not Flexibility." *Molecular Ecology* 29, no. 5: 899–911. <https://doi.org/10.1111/mec.15372>.
- Howells, E. J., V. H. Beltran, N. W. Larsen, L. K. Bay, B. L. Willis, and M. J. H. van Oppen. 2012. "Coral Thermal Tolerance Shaped by Local Adaptation of Photosymbionts." *Nature Climate Change* 2, no. 2: 116–120. <https://doi.org/10.1038/nclimate1330>.
- Hughes, T. P., J. Kerry, M. Álvarez-Noriega, et al. 2017. "Global Warming and Recurrent Mass Bleaching of Corals." *Nature* 543: 373–377. <https://doi.org/10.1038/nature21707>.
- Hume, B. C. C., E. G. Smith, M. Ziegler, et al. 2019. "SymPortal: A Novel Analytical Framework and Platform for Coral Algal Symbiont Next-Generation Sequencing ITS2 Profiling." *Molecular Ecology Resources* 19, no. 4: 1063–1080. <https://doi.org/10.1111/1755-0998.13004>.
- Johnston, E. C., R. Cunning, and S. C. Burgess. 2022. "Cophylogeny and Specificity Between Cryptic Coral Species (*Pocillopora* spp.) at Mo'orea and Their Symbionts (Symbiodiniaceae)." *Molecular Ecology* 31, no. 20: 5368–5385. <https://doi.org/10.1111/mec.16654>.
- Kassambra, A. 2018. "Survminer: Drawing Survival Curves Using ggplot2." <https://CRAN.R-project.org/package=survminer>. R package version 0.4.3.
- Klein, S. G., C. Roch, and C. M. Duarte. 2024. "Systematic Review of the Uncertainty of Coral Reef Futures Under Climate Change." *Nature Communications* 15, no. 1: 2224. <https://doi.org/10.1038/s41467-024-46255-2>.
- Lachs, L., A. Humanes, D. R. Pygas, et al. 2023. "No Apparent Trade-Offs Associated With Heat Tolerance in a Reef-Building Coral." *Communications Biology* 6, no. 1: 400. <https://doi.org/10.1038/s42003-023-04758-6>.
- LaJeunesse, T. C., J. E. Parkinson, P. W. Gabrielson, et al. 2018. "Systematic Revision of Symbiodiniaceae Highlights the Antiquity and Diversity of Coral Endosymbionts." *Current Biology* 28, no. 16: 2570–2580.e6. <https://doi.org/10.1016/j.cub.2018.07.008>.
- Lenth, R. V., B. Bolker, P. Buerkner, et al. 2023. "Emmeans: Estimated Marginal Means, Aka Least-Squares Means (Version 1.10.2) [Computer Software]." <https://cran.r-project.org/web/packages/emmeans/index.html>.
- Loya, Y., K. Sakai, K. Yamazato, Y. Nakano, H. Sambali, and R. V. Woelke. 2001. "Coral Bleaching: The Winners and the Losers." *Ecology Letters* 4: 122–131. <https://doi.org/10.1046/j.1461-0248.2001.00203.x>.
- Lüdecke, D., D. Makowski, M. S. Ben-Shachar, et al. 2021. "Performance: An R Package for Assessment, Comparison and Testing of Statistical Models (Version 0.11.0) [Computer Software]." <https://cran.r-project.org/web/packages/performance/index.html>.
- Mass, T., S. Einbinder, E. Brokovich, et al. 2007. "Photoacclimation of *Stylophora pistillata* to Light Extremes: Metabolism and Calcification." *Marine Ecology Progress Series* 334: 93–102. <https://doi.org/10.3354/meps334093>.
- McLachlan, R. H., and A. G. Grottoli. 2021. *Image Analysis to Quantify Coral Bleaching Using Greyscale Model*. Io: Protocols.
- McMurdie, P. J., and S. Holmes. 2013. "Phyloseq: An R Package for Reproducible Interactive Analysis and Graphics of Microbiome Census Data." *PLoS One* 8, no. 4: e61217. <https://doi.org/10.1371/journal.pone.0061217>.
- Mohamed, A. R., M. A. Ochsenkühn, A. M. Kazlak, A. Moustafa, and S. A. Amin. 2023. "The Coral Microbiome: Towards an Understanding of the Molecular Mechanisms of Coral–Microbiota Interactions." *FEMS Microbiology Reviews* 47, no. 2: fuad005. <https://doi.org/10.1093/femsre/fuad005>.
- Muscantine, L. 1990. "The Role of Symbiotic Algae in Carbon and Energy Flux in Reef Corals." In *Ecosystems of the World. Coral Reefs*, edited by Z. Dubinsky, vol. 25, 75–87. Amsterdam, The Netherlands: Elsevier.
- Neave, M. J., R. Rachmawati, L. Xun, et al. 2017. "Differential Specificity Between Closely Related Corals and Abundant *Endozoicomonas* Endosymbionts Across Global Scales." *ISME Journal* 11, no. 1: 186–200. <https://doi.org/10.1038/ismej.2016.95>.
- Nunes, F. L. D., R. D. Norris, and N. Knowlton. 2011. "Long Distance Dispersal and Connectivity in Amphi-Atlantic Corals at Regional and Basin Scales." *PLoS One* 6, no. 7: e22298. <https://doi.org/10.1371/journal.pone.0022298>.
- Oksanen, J., G. Blanchet, M. Friendly, et al. 2019. "Vegan: Community Ecology Package. R Package Version 2.4-6." *R Package Version* 2: 5–6.
- Palacio-Castro, A. M., T. B. Smith, V. Brandtneris, et al. 2023. "Increased Dominance of Heat-Tolerant Symbionts Creates Resilient Coral Reefs in Near-Term Ocean Warming." *Proceedings of the National Academy of Sciences* 120, no. 8: e2202388120. <https://doi.org/10.1073/pnas.2202388120>.
- Pantos, O., P. Bongaerts, P. G. Dennis, G. W. Tyson, and O. Hoegh-Guldberg. 2015. "Habitat-Specific Environmental Conditions Primarily Control the Microbiomes of the Coral *Seriatopora hystrix*." *ISME Journal* 9, no. 9: 1916–1927. <https://doi.org/10.1038/ismej.2015.3>.
- Peixoto, R. S., M. Sweet, H. D. M. Villela, et al. 2021. "Coral Probiotics: Premise, Promise, Prospects." *Annual Review of Animal Biosciences* 9, no. 1: 265–288. <https://doi.org/10.1146/annurev-animal-090120-115444>.
- Pogoreutz, C., and M. Ziegler. 2024. "Frenemies on the Reef? Resolving the Coral–*Endozoicomonas* Association." *Trends in Microbiology* 32: 422–434. <https://doi.org/10.1016/j.tim.2023.11.006>.
- Prada, C., and M. E. Hellberg. 2021. "Speciation-By-Depth on Coral Reefs: Sympatric Divergence With Gene Flow or Cryptic Transient Isolation?" *Journal of Evolutionary Biology* 34, no. 1: 128–137. <https://doi.org/10.1111/jeb.13731>.
- Prada, C., S. E. McIlroy, D. M. Beltrán, et al. 2014. "Cryptic Diversity Hides Host and Habitat Specialization in a Gorgonian–Algal Symbiosis." *Molecular Ecology* 23: 3330–3340. <https://doi.org/10.1111/mec.12808>.
- Primov, K. D., D. R. Burdick, S. Lemer, Z. H. Forsman, and D. J. Combosch. 2024. "Genomic Data Reveals Habitat Partitioning in Massive *Porites* on Guam Micronesia." *Scientific Reports* 14, no. 1: 17107. <https://doi.org/10.1038/s41598-024-67992-w>.
- Quast, C., E. Pruesse, P. Yilmaz, et al. 2012. "The SILVA Ribosomal RNA Gene Database Project: Improved Data Processing and Web-Based Tools." *Nucleic Acids Research* 41, no. D1: D590–D596. <https://doi.org/10.1093/nar/gks1219>.
- Quek, Z. B. R., and D. Huang. 2019. "Effects of Missing Data and Data Type on Phylotranscriptomic Analysis of Stony Corals (Cnidaria: Anthozoa: Scleractinia)." *Molecular Phylogenetics and Evolution* 134: 12–23. <https://doi.org/10.1016/j.ympev.2019.01.012>.
- Quek, Z. B. R., S. S. Jain, Z. T. Richards, et al. 2023. "A Hybrid-Capture Approach to Reconstruct the Phylogeny of Scleractinia (Cnidaria: Hexacorallia)." *Molecular Phylogenetics and Evolution* 186: 107867. <https://doi.org/10.1016/j.ympev.2023.107867>.

- R Core Team. 2020. "R: A Language and Environment for Statistical Computing." Vienna, Austria: R Foundation for Statistical Computing. <https://www.R-project.org/>.
- Rippe, J. P., G. Dixon, Z. L. Fuller, Y. Liao, and M. Matz. 2021. "Environmental Specialization and Cryptic Genetic Divergence in Two Massive Coral Species From the Florida Keys Reef Tract." *Molecular Ecology* 30, no. 14: 3468–3484. <https://doi.org/10.1111/mec.15931>.
- Rivera, H. E., A. L. Cohen, J. R. Thompson, I. B. Baums, M. D. Fox, and K. S. Meyer-Kaiser. 2022. "Palau's Warmest Reefs Harbor Thermally Tolerant Corals That Thrive Across Different Habitats." *Communications Biology* 5, no. 1: 1394. <https://doi.org/10.1038/s42003-022-04315-7>.
- Rose, N. H., R. A. Bay, M. K. Morikawa, L. Thomas, E. A. Sheets, and S. R. Palumbi. 2021. "Genomic Analysis of Distinct Bleaching Tolerances Among Cryptic Coral Species." *Proceedings of the Royal Society B: Biological Sciences* 288: 20210678. <https://doi.org/10.1098/rspb.2021.0678>.
- Scheufen, T., R. Iglesias-Prieto, and S. Enríquez. 2017. "Changes in the Number of Symbionts and *Symbiodinium* Cell Pigmentation Modulate Differentially Coral Light Absorption and Photosynthetic Performance." *Frontiers in Marine Science* 4: 309. <https://doi.org/10.3389/fmars.2017.00309>.
- Scheufen, T., W. E. Krämer, R. Iglesias-Prieto, and S. Enríquez. 2017. "Seasonal Variation Modulates Coral Sensibility to Heat-Stress and Explains Annual Changes in Coral Productivity." *Scientific Reports* 7, no. 1: 4937. <https://doi.org/10.1038/s41598-017-04927-8>.
- Schoepf, V., J. H. Baumann, D. J. Barshis, et al. 2023. "Corals at the Edge of Environmental Limits: A New Conceptual Framework to Re-Define Marginal and Extreme Coral Communities." *Science of the Total Environment* 884: 163688. <https://doi.org/10.1016/j.scitotenv.2023.163688>.
- Schweinsberg, M., R. Tollrian, and K. P. Lampert. 2016. "Genetic Variation in the Massive Coral *Porites lobata*." *Marine Biology* 163, no. 12: 242. <https://doi.org/10.1007/s00227-016-3022-8>.
- Scott, C. B., R. Schott, and M. V. Matz. 2024. "From Juveniles to Giants: Drivers of Holobiont Assembly in Massive *Porites*." <https://doi.org/10.1101/2024.01.09.574877>.
- Scucchia, F., P. Zaslansky, C. Boote, A. Doheny, T. Mass, and E. F. Camp. 2023. "The Role and Risks of Selective Adaptation in Extreme Coral Habitats." *Nature Communications* 14, no. 1: 4475. <https://doi.org/10.1038/s41467-023-39651-7>.
- Souter, D., S. Planes, J. Wicquart, D. Obura, and F. Staub. 2021. "Status of Coral Reefs of the World: 2020." *International Coral Reef Initiative*. <https://doi.org/10.59387/WOTJ9184>.
- Starko, S., J. Fifer, D. C. Claar, et al. 2023. "Marine Heatwaves Threaten Cryptic Coral Diversity and Erode Associations Amongst Coevolving Partners." *Science Advances* 9: eadf0954. <https://doi.org/10.1101/2023.01.07.522953>.
- Swain, T. D., E. DuBois, A. Gomes, et al. 2016. "Skeletal Light-Scattering Accelerates Bleaching Response in Reef-Building Corals." *BMC Ecology* 16, no. 1: 10. <https://doi.org/10.1186/s12898-016-0061-4>.
- Swain, T. D., S. Lax, N. Lake, H. Grooms, V. Backman, and L. A. Marcelino. 2018. "Relating Coral Skeletal Structures at Different Length Scales to Growth, Light Availability to Symbiodinium, and Thermal Bleaching." *Frontiers in Marine Science* 5: 450. <https://doi.org/10.3389/fmars.2018.00450>.
- Terán, E., E. R. Méndez, S. Enríquez, and R. Iglesias-Prieto. 2010. "Multiple Light Scattering and Absorption in Reef-Building Corals." *Applied Optics* 49, no. 27: 5032–5042. <https://doi.org/10.1364/AO.49.005032>.
- Terraneo, T. I., F. Benzoni, R. Arrigoni, et al. 2021. "Phylogenomics of *Porites* From the Arabian Peninsula." *Molecular Phylogenetics and Evolution* 161: 107173. <https://doi.org/10.1016/j.ympev.2021.107173>.
- Therneau, S. 1999. "A Package for Survival Analysis in S, v3.3-1."
- Thomas, L., N. H. Rose, R. A. Bay, et al. 2018. "Mechanisms of Thermal Tolerance in Reef-Building Corals Across a Fine-Grained Environmental Mosaic: Lessons From Ofu, American Samoa." *Frontiers in Marine Science* 4: 434. <https://doi.org/10.3389/fmars.2017.00434>.
- Thornhill, D. J., E. J. Howells, D. C. Wham, T. D. Steury, and S. R. Santos. 2017. "Population Genetics of Reef Coral Endosymbionts (*Symbiodinium*, Dinophyceae)." *Molecular Ecology* 26, no. 10: 2640–2659. <https://doi.org/10.1111/mec.14055>.
- Tisthammer, K. H., Z. H. Forsman, R. J. Toonen, and R. H. Richmond. 2020. "Genetic Structure Is Stronger Across Human-Impacted Habitats Than Among Islands in the Coral *Porites lobata*." *PeerJ* 8: e8550. <https://doi.org/10.7717/peerj.8550>.
- Van Oppen, M. J., P. Bongaerts, P. Frade, et al. 2018. "Adaptation to Reef Habitats Through Selection on the Coral Animal and Its Associated Microbiome." *Molecular Ecology* 27, no. 14: 2956–2971. <https://doi.org/10.1111/mec.14763>.
- van Woesik, R., P. Houk, A. L. Isechal, J. W. Idechong, S. Victor, and Y. Golbuu. 2012. "Climate-Change Refugia in the Sheltered Bays of Palau: Analogs of Future Reefs." *Ecology and Evolution* 2, no. 10: 2474–2484. <https://doi.org/10.1002/ece3.363>.
- Vásquez-Elizondo, R. M., L. Legaria-Moreno, M. Á. Pérez-Castro, et al. 2017. "Absorbance Determinations on Multicellular Tissues." *Photosynthesis Research* 132, no. 3: 311–324. <https://doi.org/10.1007/s11120-017-0395-6>.
- Vompe, A. D., H. E. Epstein, K. E. Speare, et al. 2024. "Microbiome Ecological Memory and Responses to Repeated Marine Heatwaves Clarify Variation in Coral Bleaching and Mortality." *Global Change Biology* 30, no. 1: e17088. <https://doi.org/10.1111/gcb.17088>.
- Voolstra, C. R., B. C. C. Hume, E. J. Armstrong, et al. 2023. "Disparate Genetic Divergence Patterns in Three Corals Across a Pan-Pacific Environmental Gradient Highlight Species-Specific Adaptation." *npj Biodiversity* 2, no. 1: 15. <https://doi.org/10.1038/s44185-023-00020-8>.
- Voolstra, C. R., J.-B. Raina, M. Dörr, et al. 2024. "The Coral Microbiome in Sickness, in Health and in a Changing World." *Nature Reviews Microbiology* 22: 460–475. <https://doi.org/10.1038/s41579-024-01015-3>.
- Wang, S., E. Meyer, J. K. McKay, and M. V. Matz. 2012. "2b-RAD: A Simple and Flexible Method for Genome-Wide Genotyping." *Nature Methods* 9, no. 8: 808–810. <https://doi.org/10.1038/nmeth.2023>.
- Weis, V. M. 2008. "Cellular Mechanisms of Cnidarian Bleaching: Stress Causes the Collapse of Symbiosis." *Journal of Experimental Biology* 211: 3059–3066. <https://doi.org/10.1242/jeb.009597>.
- Winters, G., R. Holzman, A. Blekhan, S. Beer, and Y. Loya. 2009. "Photographic Assessment of Coral Chlorophyll Contents: Implications for Ecophysiological Studies and Coral Monitoring." *Journal of Experimental Marine Biology and Ecology* 380: 25–35. <https://doi.org/10.1016/j.jembe.2009.09.004>.
- Ziegler, M., C. G. B. Grupstra, M. M. Barreto, et al. 2019. "Coral Bacterial Community Structure Responds to Environmental Change in a Host-Specific Manner." *Nature Communications* 10, no. 1: 3092. <https://doi.org/10.1038/s41467-019-10969-5>.
- Ziegler, M., F. O. Seneca, L. K. Yum, S. R. Palumbi, and C. R. Voolstra. 2017. "Bacterial Community Dynamics Are Linked to Patterns of Coral Heat Tolerance." *Nature Communications* 8: 1–8. <https://doi.org/10.1038/ncomms14213>.

Supporting Information

Additional supporting information can be found online in the Supporting Information section.